**Immunol Genet J, Vol. 8, No. 4, 2025, pp.332-356** **DOI: https://doi.org/10.18502/igj.v8i4.20101**

**Original Article**

# Design of a Trivalent DC-inducing mRNA Vaccine Against Monkeypox, Cowpox, and Vaccinia Viruses: A Computational Approach

**Cena Aram[1,2†], Kiarash Saleki[3,4,5†], Amirreza Mazloomi[4], Nima Rezaei[5,6*]**

*[1] Department of Cell & Molecular Biology, Faculty of Biological Sciences, Kharazmi University, Tehran, Iran*

*[2] Universal Scientific Education and Research Network (USERN), Babol, Iran*

*[3] Research Center for Immunodeficiencies, Children's Medical Center, Tehran University of Medical Sciences, Tehran, Iran*

*[4] Student Research Committee, Babol University of Medical Sciences, Babol, Iran*

*[5] Network of Immunity in Infection, Malignancy and Autoimmunity (NIIMA), Universal Scientific Education and Research Network (USERN), Tehran, Iran*

*[6] Department of Immunology, School of Medicine, Tehran University of Medical Sciences, Tehran, Iran*

*†Co-first authorship and contributed equally.*

Received: 11 July 2025; Accepted: 18 November 2025

## Abstract

**Background:** Monkeypox virus (MPXV) is a novel virus that has been disseminated around the globe and caused human disease. Over 86 thousand infection cases have been reported, which has concerned the World Health Organization (WHO). Given the challenges faced due to the spread of MPXV, an immune-mediating therapy to prevent infection by MPXV is invaluable to aid large-scale public health practices. In this field, the mRNA vaccine could be a sufficient way to control the virus's transmissibility around worldwide study; we used immunoinformatic approaches that aided the pathway to develop the novel mRNA vaccine.

**Methods:** In the first step, we gathered three key proteins (A35R, cell surface binding, and M1R) conserved in Cowpox as well as Vaccinia viruses for the design of vaccines and computed the potent immunogen epitopes that the engineered vaccines assemble with the fused finalized epitopes and Beta-defensin 3 adjuvant that is a major stimulation of dendritic cells (DCs), along with the PADRE and TAT sequences were added. The vaccine construct was modeled with Robetta tool and validated by PROCHECK, ERRAT, and Z-score. Physicochemical properties were also investigated and confirmed to be favorable. Disulfide engineering, immunological simulation, and molecular docking with TLR3 were performed. Finally, the construction of mRNA was designed in silico, the mRNA vaccine structure was predicted, and then the molecular dynamics simulation was performed to investigate the TLR3-vaccine complex.

**Results:** The eighteen final epitopes were predicted. The engineered multi-epitope protein, entails 350 amino acids and had good structural quality, as quantified through an ERRAT value over 99%. Also, engineering of disulfide bond was performed in order to augment the construct stability of the MPXV vaccine. The Ramachandran analysis was utilized to further corroborate the favorable φ (phi) and ψ (psi) angles, with the aminoacids localized to the highly favorable or permitted regions. The design of the mRNA construct was achieved by incorporating the 5'UTR, start codon, signal peptide, open reading frames, stop codon,3'UTR, and polyA. In addition, the immune simulation showed sustained immune response. Also, the molecular dynamic simulation (MDS) and energy analyses suggested that the vaccine-TLR3 complex binding was stable.

**Conclusion:** An mRNA vaccine was designed to provoke a robust immune response against MPXV while offering immunoprotection against Cowpox and Vaccinia. The present work analyzed the structure of a novel multi-epitope vaccine, which indicated it could be an effective option against MPXV infection. Future study is recommended to confirm the immunomodulatory role of the designed MPXV vaccine.

**Keywords:** Computational Immunology; Immunoinformatic; Monkeypox; Molecular Dynamics; Polytopic Vaccine; Reverse Vaccinology

***Corresponding Author:** Nima Rezaei, MD, PhD

Research Center for Immunodeficiencies, Pediatrics Center of Excellence, Children's Medical Center Hospital, Tehran University of Medical Sciences, Tehran, Iran

E-mail: rezaei_nima@tums.ac.ir

**How to cite this article**

*Aram C, Saleki K, Mazloomi A, Rezaei N. Design of a Trivalent DC-inducing mRNA Vaccine Against Monkeypox, Cowpox, and Vaccinia Viruses: A Computational Approach. Immunol Genet J, 2025; 8(4): 332-356.* DOI: https://doi.org/10.18502/igj.v8i4.20101

## Introduction

Infection by the monkeypox virus (MPXV) affects both animals and humans (1). The monkeypox virus (MPXV) is a member of the Orthopoxvirus genus of the Poxviridae family. It has a double-stranded (ds) DNA genome with 197 kilobases (kb) in length and encodes about 190 open reading frames (ORFs). MPXV ORFs direct viral replication within the host cells (2). The formation of MPXVs is oval or brick-shaped, with dimensions measuring 200 by 250 nm (3). Other members of the orthopoxvirus genus are vaccinia virus (VACV), cowpox virus (CPXV), smallpox virus (SPXV), and several other animal pathogen poxviruses (4).

MPXV first emerged in a monkey. Later, the first human infection dates back to 1970 in Congo, where it rapidly caused an endemic and disseminated throughout Africa (5). The current monkeypox outbreak, which was initially reported in Europe in a limited number of human cases in early 2022 has been linked to global warming and numerous effects on the weather in the world (6). As of 2023, 86,746 confirmed cases and 112 deaths had been reported globally. By then, at least 100 nations had recorded the dissemination of MPX. Intriguingly, the WHO has estimated mortality rates of about 3-6% from monkeypox in spite of historically increased death rates (7).

The symptoms of MPXV include fever, rash, headache, flu, and lymphadenopathy (8). Extracellular enveloped virus (EEV) and intracellular mature virus (IMV) are the two most contagious types of MPXV (9). MPXV is primarily spread through close contact with an infected individual. Most cases that contract MPXV recover within 2 weeks to 1 month. Currently, there is no verified therapy for MPX in the US. Nevertheless, Tecovirimat, which is an antiviral medication, is a potentially suitable option for the treatment of certain cases influenced by MPXV (10,11).

According to recent research, in mice, immunization with DNA encoding L1R (an IMV protein) and A33R led to the development of neutralizing antibodies against L1R and IgGs against A33R (12). An innovative mRNA vaccine that expresses a fusion protein made of the extracellular domain of monkeypox A35R, and the M1R has recently been shown to be efficient in inducing both cellular and humoral immunities against the viral infection (13). M1R (myristoylated surface membrane protein of IMV), an anscestrally conserved protein which is important for virion assembly and cell entry (14). In a similar fashion to the VACV A33R, research has shown A35R is an envelope glycoprotein capable of inducing actin-rich microvilli and promoting efficient transfer of viral particles between cells.

The field of immunotherapy design is fast-moving, with biological therapies, CAR T-cells, and the design of novel vaccine technologies (15–17). To develop vaccines, candidate pathogen secretory proteins must predict B and T cell epitopes (18,19), such as cell surface binding protein, A33R, and L1R. However, the Food and Drug Administration in the US approved the Jynneos vaccine against monkeypox and smallpox experimentally, which is safe for prevention (20). In the future, it may decrease its efficacy if the virus mutates (21), and ACAM2000 provided the protective vaccine with around 85% effectiveness against MPXV (22). Experiences associated with the COVID-19 mRNA vaccine highlighted the significance of high-quality mRNA vaccines in preventing viral infection, such as Moderna and Pfizer-BioNTech showed the efficiency of the new generation of vaccine (23).

The comparison of different research based on immunoinformatics approaches is helping to progress the vaccine product and keep on experiments in vivo (24,25). Several immunoinformatics approaches that designed the different multi-epitope vaccines against MPXV that were used in this research (26,27). The mRNA-based vaccines are a novel type of vaccines against cancer and infectious pathogens (28). Compared to DNA-based vaccinations, mRNA vaccines have greater biosafety characteristics because antigen or multi-epitope translation takes place in the cytoplasm (29).

Moreover, mRNA vaccines can be adjuvanted and bind to pattern-recognition receptors (30). Taking into account the implications of such virulence, our research aimed to design and engineer an mRNA multi-epitope vaccine which could potentially provoke humoral as well as cell-modulated immunological responses targetting MPXV. In this line, we focused on indicated immunogenic epitopes extracted from three important target proteins, namely cell surface bind-

ing protein, A35R, and M1R. The major aspects of these proteins in the virus's infectivity and immune evasion render them optimal candidates for immune-mediating treatment development. It was a comprehensive computational study wherein we selected Immunoinformatics tools for epitope detection and prioritization of the vaccine candidates with considerable immunogenic potential. This work is novel in engineering a trivalent mRNA vaccine that shows MPXV, CPXV, and VACV-conserved epitopes. Through targeting key conserved epitopes, the designed immunotherapy may trigger broad protective immunological responses towards MPXV as well as closely associated orthopoxviruses, including CPXV and VACV. This cross-immunoprotective feature is in particular useful for the mitigation of outbreaks linked to zoonotic orthopoxviruses and for complementing preparedness against future poxvirus pathogen outbreaks. Additionally, this computational method will also warrant the selection of highly immunogenic and non-allergic epitopes, as a result, maximizing the safety and efficacy of the immunogenic candidate. It is also crucial to understand the induction of two branches of adaptive immune response (humoral as well as cell-mediated), which additionally enhances its long-lasting immune response. Overall, the results of the present work constitute significant clues that help vaccine design strategies against MPXV and for the emerging and re-emerging poxvirus infections.

## Materials and Methods

### Extracting Proteins, validation, prediction of epitope, and identifying the conservation of epitopes in Cowpox/Vaccinia virus

The sequence of 3 proteins of Monkeypox (A35R (NCBI Accession Number: AGR35269.1), Cell surface-binding protein (Uniprot Accession Number: A0A0F6N859), and M1R (Uniprot Accession Number: QJQ40223.1)) was extracted from National Center for Biotechnology Information (NCBI) and uniport. The VaxiJen server, which has viral module functionality, was used to test the antigenicity of proteins (http://www.ddg-pharmfac.net/vaxijen/VaxiJen/VaxiJen.html). For the mentioned purpose, Immune Epitope Database (IEDB) online server (http://tools.iedb.org/mhci/, http://tools.iedb.org/mhcii/) is used for the prediction of CTL and HTL with the IEDB recommended method and frequent alleles. The workflow chart of the research is demonstrated in **Figure 1**. At last, we searched the epitopes in Blastp to identify the similarity of the epitopes with Cowpox and vaccinia virus proteins.

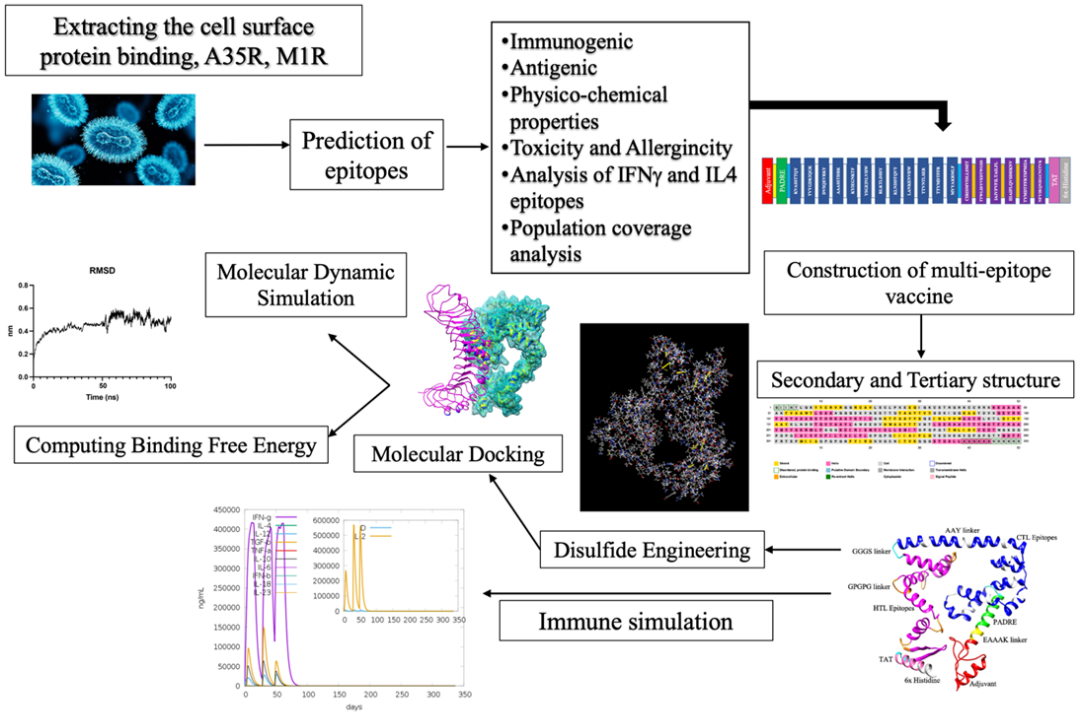


**Figure 1.** The pathway of designing of mRNA vaccine based on multi-epitopes against the Monkeypox virus.

**Construction and characterization of multi-peptide**

After the prediction of immunogen epitopes for the A35R, cell surface-binding protein, and M1R proteins, we used the various linkers to bond the candidate epitopes for designing a monkeypox multi-epitope vaccine. The CTL and HTL epitopes were linked using EAAAK, GGGS, GPGPG, and AAY linkers. These immunogenic linkers aid in the development of vaccines that increase immune responses. After that, the use of human Beta-defensin 3, that are antimicrobial peptide and has a role in the maturation of human Langerhans cell-like dendritic cells, and Th1 to enhance immune responses that have an important role in innate immune response (31,32). Beta-defensin 3 was added to the N-terminal of the vaccine construct, and the EAAAK linker linked the PADRE sequence (13 aa) to increase the immunogenicity (33), then the GGGS linker connected CTL and HTL epitopes. The CTL epitopes linked with AAY and the HTL were linked by GPGPG, and at the C-terminal, TAT and 6x-Histidine were added, as demonstrated in **Figure 1**. In addition, the evaluation of the multi-epitope vaccine used Protparam tools (https://web.expasy.org/protparam/) to assess physico-chemical properties such as half-life, theoretical PI, molecular weight, and grand average of hydropathy (GRAVY). We assessed antigenicity, toxicity, and allergenicity of multi-epitope vaccine using Vaxijen (34) and ANTIGENpro (https://scratch.proteomics.ics.uci.edu/), Toxinpred (35), Algpred (36) servers. Blastp has been employed in the study of human protein epitopes for non-homology to avoid autoimmune reactions (37).

**Analysis of IFNγ and IL4 epitopes in multi-epitope vaccine**

Interferon-gamma (IFNγ) is the main cytokine for innate and adaptive immunity against viral infection (38). IFNγ is a crucial macrophage activator and inducer of the production of the MHC II protein (39) Interleukin-4 has a critical role in the stimulation of activated B cells and T cells, and B cells to plasma cell differentiation. In this case, for analyzing the multi-epitope sequence using IFNepitope (https://webs.iiitd.edu.in/raghava/ifnepitope/scan.php) and IL4pred (https://webs.iiitd.edu.in/raghava/il4pred/scan.php) server to detect the position of IFNγ and IL4 inducer, we used IFNepitope with the SVM algorithm, and the other option was the default. As well as, for IL4pred using the default setting.

**Secondary and tertiary structure prediction with evaluation of a multi-epitope vaccine**

To predict secondary structure utilized PSIPRED (http://bioinf.cs.ucl.ac.uk/psipred/) and SOPMA (https://npsa-prabi.ibcp.fr/cgi-bin/npsa_automat.pl?page=/NPSA/npsa_sopma.html) server to calculate the percentage of Helices (H), stand (S), and Coil (C). Then, DISORDER3 in PSIPRED was carried out to predict the disorder sites. Furthermore, for the prediction of the tertiary structure of the multi-epitope vaccine implemented, the Robetta server (https://robetta.bakerlab.org/) was used for 3D structure modeling. Robetta is a server for the prediction of protein structure based on Continuous Automated Model Evaluation (CAMEO) (40). Afterward, to validate the quality of the 3D structure multi-epitope vaccine used online validation ProsA-web server (https://prosa.services.came.sbg.ac.at/prosa.php), PROCHECK, and ERRAT (https://saves.mbi.ucla.edu/) for analyzing the structure of multi-epitope vaccine.

**Engineering of the Disulfide bond**

Disulfide engineering is an important field that aids in the development of multi-epitope constructs and improves the quality and stability of protein constructs that utilize the disulfide engineering approach to improve the stability of protein constructs. Disulfide engineering was performed in this field using Disulfide by Design v2.0 (http://cptweb.cpt.wayne.edu/DbD2/index.php) for amino acid mutation into cysteine for the formation of unique disulfide bonds in the manufactured vaccine. In addition, we compared the quality of the constructed vaccine after engineering the disulfide bond with ProsA-web, PROCHECK, and the ERRAT server.

**Linear and discontinuous B-cell epitope prediction**

In this work, we estimated discontinuous and linear B-cell epitopes in 3D structure using the ElliPro online server (http://tools.iedb.org/elipro), and the analysis of different methods has been

proceeding in BCEpred (https://webs.iiitd.edu.in/raghava/bcepred/bcepred_submission.html) this method predicted the continuous or linear B-cell epitopes from various physicochemical properties such as accessibility, hydrophilicity, antigenic propensity, exposed surface, flexibility, turns, and polarity.

**Molecular Docking of TLR3 and constructed vaccine**

The study of molecular docking was run to investigate the interaction and binding between immune receptors, such as toll-like receptor 3 (TLR3) (41,42). For this purpose, an online server HDOCK (http://hdock.phys.hust.edu.cn/) was employed (43), which TLR3 (PDB ID: 2a0z) was downloaded from RCSB and got ready for molecular docking that Chimera UCSF v1.16 used in this study. To demonstrate the interaction such as salt bridge, hydrogen bond, and non-bonded contact utilized PDBsum generate a server (44).

**Norm mode analysis**

The conformational stability of the TLR3-vaccine complex was studied with iMODS server (http://imods.ch aconlab.org). The server represents NMA mobility, B-factor, Ei-genvalues, linkage matrix, variance, and covariance map. The analysis supports us in indicating the dynamic motion and rigidity of the complex's construction.

**Molecular Dynamics simulation and binding free energy**

The molecular dynamic simulation of the constructed vaccine and TLR3 complex was achieved using the GROMACS version 2023 software, and VMD was used to visualize and confirm the encircled TLR3-vaccine complex for detecting the molecular dynamic system. The OPLS-AA force field and the creation of the system included the solvent (TIP3P) and 0.15 concentration of salt to peruse the simulation in blood osmolarity and the complex centered in a triclinic box (45). The minimization of the TLR3 vaccine was Fmax<1000 kJ/mol nm, and that included the NVT and NPT stabilization continually. The fever temperature state was patterned to use the 310 K◦ and 1 Bar pressure with Berendsen thermostat that approached the real situation in the blood that the pressure and the temperature state set to 100 picoseconds. The MD run was conducted for 100 ns. The complex was prepared by energy minimization, NVT, and NPT steps, and the production 100-ns MD run which produced the final trajectory. Finally, we calculated the Root-mean-square deviation (RMSD), Root-mean-square fluctuation (RMSF), and gyration.

**Computing the Binding Free Energy with MM/GBSA Method**

The HawkDock web server (http://cadd.zju.edu.cn/hawkdock/) was used to compute the binding free energy (ΔG) for TLR4-vaccine before and after 10 ns MD simulation. Molecular Mechanics/Generalized Born Surface Area (MM/GBSA) is the trustworthy method that calculated the Delta G (46). The formula of this method follows;

$$\Delta Gbind = \Delta EMM + \Delta GGB + \Delta GSA - T\Delta S \quad (1)$$

$$\Delta EMM = \Delta Einternal + \Delta Eelectrostatic + \Delta Evdw \quad (2)$$

**Codon Optimizations and mRNA Construction**

The multi-peptide vaccine construct requires to adapt for codon optimization for adequate expression in the host cell of humans. We used JCAT (Java Codon Adaption Tool) server (47) to optimize the codon for humans. The construction of mRNA patterned from Moderna mRNA-1273 vaccine against SARS-CoV-2 that the sequence of that vaccine extracted from NCBI (OK120841.1) that MPXV mRNA vaccine consists of 5' m7G-Cap, 5' Untranslated regions (5'UTR) (48), Start Codon (49) Signal Peptide, Open Reading Frame (ORF), Stop Codon, 3'UTR-PolyA (50) that PolyA improves mRNA stability, translational activities and avoid from nuclease degradation (51). In addition, for the prediction of the mRNA vaccine construct was used the mfold server (http://www.unafold.org/mfold/applications/rna-folding-form.php).

**Immune Simulation**

The C-ImmSim web server (http://150.146.2.1/C-IMMSIM/index.php) was used to model the immunological response to a multi-epitope vaccination. In this study, we simulated vaccine injection without LPS and selected the 3 injections at

time steps 1, 84, and 144 to evaluate the immune response over 11 weeks. The simulation steps were used 1010, and the other option was in the default setting.

### Population Coverage Analyzing

The discovery of population coverage about multi-epitope vaccine, the vaccine epitopes with corresponding HLA alleles were added into the population coverage analysis of IEDB (http://tools.iedb.org/population/) that some locations were selected for this analysis such as Europe, Asia, Africa, America, and world analysis. In addition, we selected classes I and II combined for our analysis, and the rest of the options were default.

### MHC Cluster Analysis

In the majority of animals, the MHC genetic region exhibits high polymorphism. Most MHC molecules still have their unique specificity uncharacterized. Based on their projected binding specificity, MHC class I molecules (MHC I) are functionally clustered using the MHC cluster tool (52). The program offers graphical tree-based and heat-map-based depictions of the functional link between MHC class I and class II variations that are incredibly easy to understand. This study utilized the MHCcluster server. The setting for MHC I included the HLA prevalent and highly frequent MHC alleles, and for MHC II, used the HLA-DR representatives (DRB1_1501, DRB3_0101, DRB1_0701, DRB4_0101, DRB1_1402, DRB1_1101, DRB1_0803).

## Result

### Validation of protein and Prediction of epitope

Twelve MHC I epitopes were forecasted using the IEDB server (each with a percentile rank ≤ 0.05). From each protein (A35R, cell surface binding, and M1R), four epitopes were chosen. Moreover, six MHC II epitopes were selected to augment the stimulation of the innate immune response, as described in detail in Table 1. The antigenicity score of A35R, cell surface binding, and M1R showed 0.49, 0.53, and 0.63, respectively. In order to analysis of Blastp of epitopes showed that the A35R epitopes is related to CPXV168 and EEV glycoprotein, in CPXV and VACV that demonstrated in **Figure 2**.

### Construction and validation of a multi-epitope vaccine

We used 12 CTL and 6 HTL based on a high prediction score **(Table 1)**. The final step for designing the Monkeypox vaccine was the insertion of all the predicted immunogenic epitopes for A35R, Cell surface binding, and M1R that were linked with different linkers. The AAY, GPGPG, and GGGS linkers were utilized to combine CTL

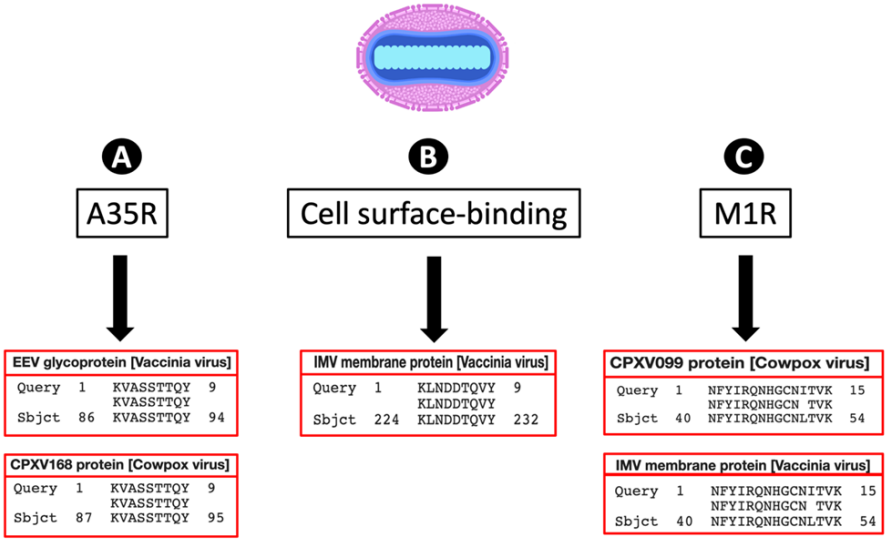


**Figure 2.** The Blastp analysis of the proteins from cowpox and the vaccinia virus revealed that the A35R, cell-binding, and M1R epitopes are all conserved. (A) The T-cell epitopes that are conserved with EEV glycoprotein and CPXV168. (B) IMV membrane protein of Vaccinia virus is conserved with cell surface-binding protein. (C) T-cell epitope of M1R is conserved with CPXV099 and IMV membrane proteins.

**Table 1.** The candidate of T lymphocyte epitopes (CTL and HTL epitopes) and their related MHC alleles

| Protein | MHC I Epitope | Allele | Position | Percentile Rank | Homology in Cowpox and Vaccinia Virus |
|---|---|---|---|---|---|
| A35R | KVASSTTQY<br>TVYGDKIQGK<br>DVSQEVRKY<br>AAASSTHRK | HLA-A*30:02<br>HLA-B*15:01<br>HLA-A*03:01<br>HLA-A*01:01<br>HLA-A*11:01 | 86-94<br>17-26<br>170-178<br>78-86 | 0.01<br>0.04<br>0.02<br>0.03 | Homology with the CPXV168 protein and EEV glycoprotein |
| Cell surface-binding protein | KYIEGNKTF<br>YSGEINLVHW<br>RLKTLDIHY<br>KLNDDTQVY | HLA-A*24:02<br>HLA-A*23:01<br>HLA-B*15:01<br>HLA-A*01:01 | 268-276<br>87-96<br>20-28<br>224-233 | 0.01<br>0.04<br>0.01<br>0.02 | Homology with IMV membrane protein and carbonic anhydrase |
| M1R | LANKENVHW<br>TTVNTLSER<br>TTYMDTFFR<br>MYYAKRMLF | HLA-B*58:01<br>HLA-B*57:01<br>HLA-A*68:01<br>HLA-A*23:01 | 220-228<br>9-17<br>229-237<br>201-209 | 0.01<br>0.01<br>0.02<br>0.01 | Homology with IMV membrane protein and CPXV099 protein |
| **Protein** | **MHC II Epitope** | **Allele** | **Position** | **Percentile Rank** | **Homology in Cowpox and Vaccinia Virus** |
| A35R | CIRISMVISLLSMIT<br>TTWLIDYVEDTWGSD | HLA-DRB1*15:01<br>HLA-DRB3*01:01 | 36-50<br>141-155 | 0.7<br>0.9 | Homology with the CPXV168 protein and EEV glycoprotein |
| Cell surface-binding protein | IAIVFVFILTAILFL<br>IIIAIFLQVSDHKNV | HLA-DRB1*07:01<br>HLA-DRB4*01:01 | 279-293<br>115-129 | 0.12<br>0.59 | Homology with IMV membrane protein and carbonic anhydrase |
| M1R | TYMDTFFRTSPMIIA<br>NFYIRQNHGCNITVK | HLA-DRB1*07:01<br>HLA-DRB3*02:02 | 230-244<br>40-54 | 0.27 | Homology with IMV membrane protein and CPXV099 protein |

and HTL epitopes. At the N-terminal, we added Adjuvant Human Beta defensin 3, and the PADRE sequence was inserted, and the immunogen CTL and HTL were connected with the GGGS linker, and at the C-terminal, we inserted the TAT sequence and 6H-Histidine. The general construction is Adjuvant-EAAAK-PADRE-GGGS-CTL-AAY-CTL-GGGS-HTL-GPGPG-HTL-GGGS-TAT-HHHH. In addition, the assessment of the multi-epitope vaccine showed in **Table 2**, explained the stability, Allergenicity, Toxicity, Antigenicity, and other physico-chemical properties.

**Table 2.** The physicochemical properties and measurement of trivalent mRNA vaccine.

| Property | Measurement |
|---|---|
| **Molecular weight** | 38,021.60 Da |
| **Formula** | C1719H2638N468O480S15 |
| **Theoretical pI** | 9.47 (Basic) |
| **Ext. coefficient** | 66,740 $M^{-1}$ $cm^{-1}$ |
| **Instability index** | 31.73 (Stable) |
| **Aliphatic index** | 77.66 (Thermostable) |
| **Half-Life** | 30 hours (mammalian reticulocytes, in vitro) >20 hours (yeast, in vivo) >10 hours (Escherichia coli, in vivo) |
| **Antigenicity** | ANTIGENpro (0.799), VexiJen v2.0 (0.46) |
| **Toxicity** | Non-Toxin |
| **Allergenicity** | Non-Allergen |
| **GRAVY** | -0.071 (Hydrophilic) |

**Analysis of IFNγ and IL-4 epitopes in mRNA vaccine based on multi-epitope**

The analysis of the multi-epitope vaccine predicted epitopes that can stimulate IFNγ and IL-4, as shown in **Figure S1**. We gathered the epitopes and characterized the region of the epitopes. We Discovered the IFNγ that predicted 149 epitopes that induced IFNγ and the length of epitope was 15 at positions 24-71,62-78, 68-83, 74-90, 89-114, 74-96, 71-86, 100-116, 133-154, 160-183, 185-200, 189-206, 193-211, 209-228, 215-230, 246-272, 260-288, 306-325, 312-329, 316-350.

**Prediction of secondary structure, modeling, and 3D structure validation**

We carried out the secondary structure analysis by PSIPRED and SOPMA and predicted the alpha-helix percent, beta-sheet, and random coil, which is shown in **Figure 3**. The structure contains 39.71% alpha-helix, 23.14 beta-sheet, and 37.14% random coil. The 3D structure and construction of the multi-epitope vaccine were indicated in **Figure 4**, and we used the Robetta server for the prediction of the tertiary structure of the vaccine. The validation of the tertiary structure of the multi-epitope vaccine was performed by PROCHECK, ERRAT, and Z-score that validated and the result has shown the (92.3%) 277 residues in most favored regions, 16 residues (5.3%) in additional allowed regions, 3 residues (1%) in generously allowed regions, and 4 residues (1.3%) in disallowed regions that got in Ramachandran plot and the ERRAT analysis showed 99.115 scores that have a high quality in prediction of tertiary structure and also the Z-score showed the 6.02 score **(Figure 3)**.

**Disulfide bond**

Disulfide engineering was used to stabilize the structure. The energy value of chi3 varied from -87 to +97, indicating that suitable residues change into cysteine. Furthermore, Analysis of identified residue pairs for variation and engineering of disulfide bonds includes CYS23-39LYS, GLY66-GLY131, ALA106- LEU135, ALA140-ILE148, ALA152-GLN160, LEU267-GLY274, MET306-THR317, PHE316, ALA336, GLN320-CYS324. The variation of structure is demonstrated in **Figure 5**. Furthermore, tertiary structure's quality was improved and the stability of construction

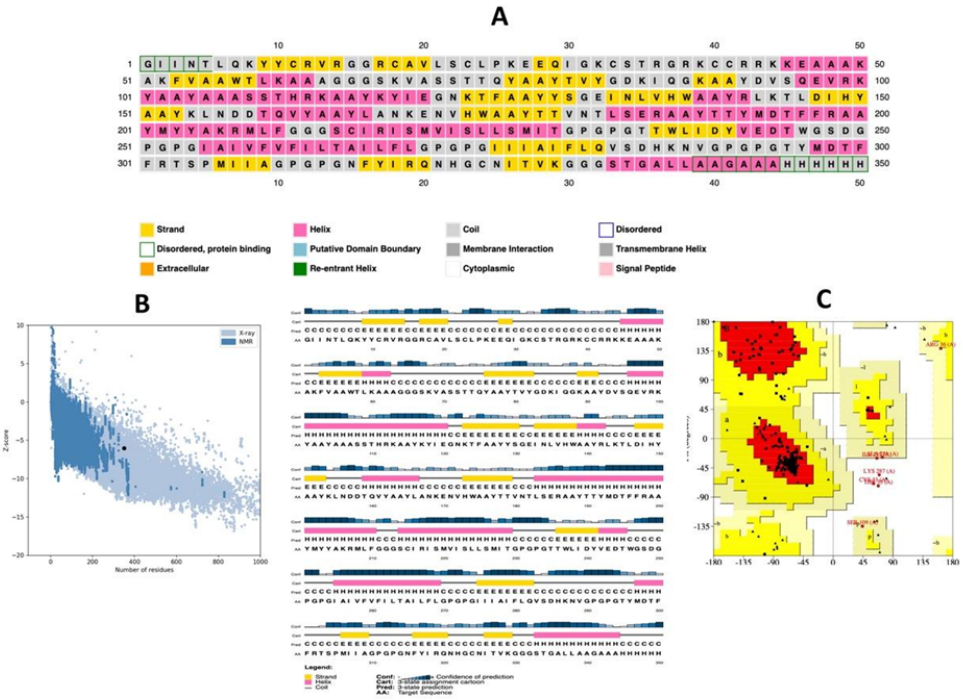


**Figure 3.** Estimation of the MPXV's 2D structure and tertiary structure validation. (A) The PSIPRED server predicted the secondary structure of the multi-epitope vaccination (B) Z-score validation that showed the quality of tertiary structure (C) Ramachandran plot that demonstrated the residues in the most favored region.

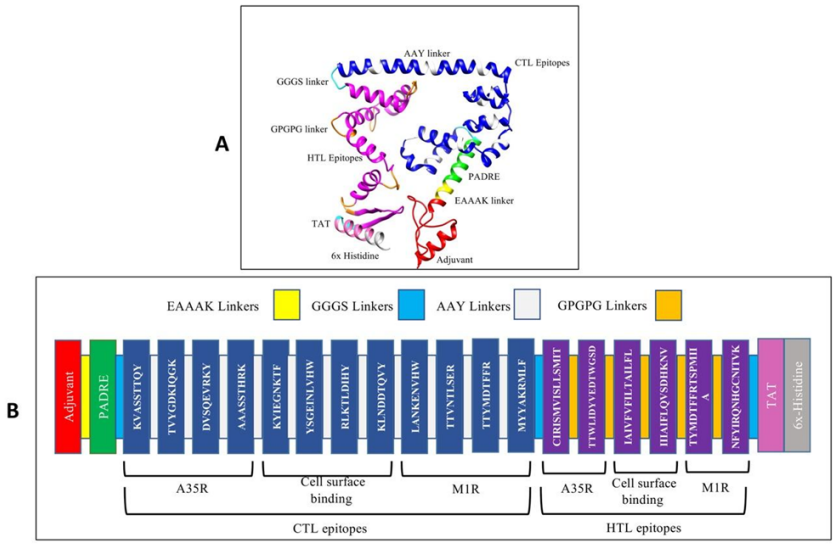


**Figure 4.** The 3D structure of the MPXV mRNA vaccine is based on a multi-epitope construct. (A) 3D structure of MPXV vaccine or product of mRNA vaccine structure (B) Construction of a multi-epitope that consists of CTL epitopes and HTL epitopes.

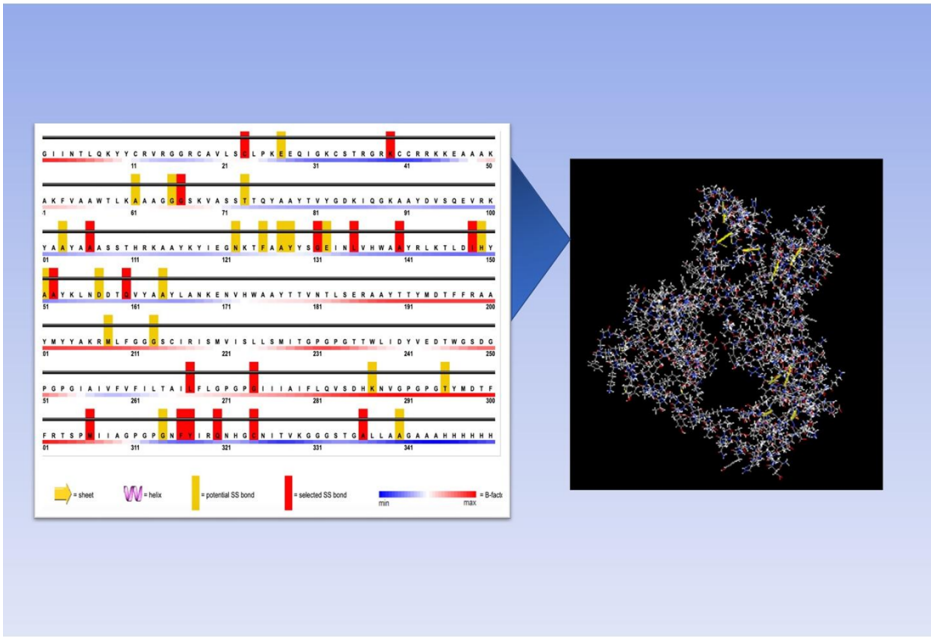

**Figure 5.** The MPXV vaccine is suitable for disulfide bond engineering.
Disulfide bond engineering was performed by changing suitable amino acids to Cysteine, which may have resulted in a more stable design.

increased so the Z-score grow up to 6.25.

## Prediction of linear and conformational B-cell epitopes

We anticipated linear and discontinuous B-cell epitopes by Ellipro and BCEpred online server, which are gathered in **Table 3,4**, and **Figure 6**. The multi-epitope vaccine structure showed the location of discontinuous epitopes.

## Molecular docking with TLR3-vaccine

Role of innate immune elements such as Toll-like receptors (TLRs) and inflammasomes (53–55). The interaction of a Toll-like receptor (TLR) is crucial for the carriage of antigenic molecules and the stimulation of the immune response. The result of docking showed the modeled vaccine has significant interaction with TLR3 that predicted

**Table 3.** The contentious and discontinuous B-cell epitopes.

| No | Position | Continuous B-cell epitopes | score | No | Discontinuous B-cell residues | Number of residues | score |
|---|---|---|---|---|---|---|---|
| **1** | 191-219 | TYMDTFFRAAYMYYAKRMLFGG GSCIRIS | 0.779 | 1 | B:A309, B:G310, B:P311, B:G312, B:P313, B:G314, B:N315, B:C316, B:T327, B:V328, B:K329, B:G330, B:G331, B:G332, B:S333, B:T334, B:G335, B:C336, B:L337, B:L338, B:A339, B:A340, B:G341, B:A342, B:A343, B:A344, B:H345, B:H346, B:H347, B:H348, B:H349, B:H350 | 32 | 0.774 |
| **2** | 1-22 | GIINTLQKYYCRVRGGRCAVLS | 0.753 | 2 | B:F196, B:A199, B:A200, B:Y201, B:M202, B:Y203, B:Y204, B:A205, B:K206, B:R207, B:M208, B:L209, B:F210, B:G211, B:G212, B:G213, B:S214, B:C215, B:I216, B:R217, B:I218, B:S219, B:D240, B:E243, B:D244, B:T245, B:W246, B:G247, B:S248, B:D249, B:G250, B:P251, B:G252, B:P253, B:G254, B:I255, B:A256, B:V258, B:F261, B:I262, B:A265, B:I266, B:F268, B:L269, B:G270, B:P271, B:G272, B:I275 | 48 | 0.741 |
| **3** | 139-150 | ACYRLKTLDCHY | 0.725 | 3 | B:G64, B:G65, B:A114, B:A115, B:Y116, B:K117, B:Y118, B:I119, B:E120, B:G121, B:N122, B:K123, B:T124, B:F125, B:Y128, B:A139, B:C140, B:Y141, B:L143, B:K144, B:T145, B:L146, B:D147, B:C148, B:H149, B:Y150, B:V161, B:Y162, B:A163, B:A164, B:Y165, B:L166, B:A167, B:N168, B:K169, B:E170, B:N171, B:V172, B:H173, B:W174, B:A175, B:A176, B:Y177, B:T178, B:T179, B:V180, B:N181, B:S184, B:E185 | 49 | 0.726 |
| **4** | 113-125 | KAAYKYIEGNKTF | 0.721 | 4 | B:G1, B:I2, B:I3, B:N4, B:T5, B:L6, B:Q7, B:K8, B:Y9, B:Y10, B:C11, B:R12, B:V13, B:G15, B:G16, B:R17, B:C18, B:A19, B:V20, B:L21, B:S22, B:C23, B:E28, B:Q29, B:I30, B:G31, B:K32, B:C33, B:S34, B:T35, B:R36, B:G37, B:R38, B:C39, B:C40, B:C41 | 36 | 0.716 |
| **5** | 309-316 | AGPGPGNC | 0.71 | 5 | B:A188, B:T191, B:Y192, B:D194, B:T195, B:R198 | 6 | 0.637 |
| **6** | 243-256 | EDTWGSDGPGPGIA | 0.684 | | | | |
| **7** | 28-41 | EQIGKCSTRGRCCC | 0.669 | | | | |
| **8** | 265-272 | AICFLGPG | 0.644 | | | | |

the 10 poses that can bind to TLR3 as well as done. The molecular docking top score showed -352.51 with a 0.98 confidence score and 87.41 ligand RMSD (Å), which was selected. Thus, the analysis of the interaction between immune receptors performed with the PDBsum server demonstrated interface contact of vaccine-TLR3 that included one salt bridge, 14 hydrogen bonds, and 219 non-bonded contacts, as shown in **Figure 7**. The hydrogen bond residues with vaccine-TLR3 are: TYR10-TYR123, ARG42-ASN148, LYS329-THR166, TYR79-ARG222, TYR76-ARG251, TYR76-ASN252, TYR79-ASN275, LYS89-ASN275, SER72-GLU301, SER71-GLU301, GLN75-GLU301, LYS68-TYR302, SER72-TYR302, and SER72-TYR302 that having bond distance< 3.19 Å.

**Norm mode analysis (NMA)**

NMA was then conducted using the iMODs

**Table 4.** Physico-chemical Continuous B-cell epitopes

| Prediction parameter | Epitope sequence |
|---|---|
| **Hydrophilicity** | GKCSTRGRK, RRKKEAA, AAGGGSK, ASSTHRKA, KLNDDTQVY, TGPGPGTT, EDTWGSDGPGPG, QVSDHKNVG, RQNHGCN, KGGGSTGA |
| **Flexibility** | YYCRVRG, EQIGKCSTRGRKRRKK, KAAAGGGSKVA, YDVSQEV, AAASSTH, DTWGSDGP, NITVKGGGS |
| **Accessibility** | INTLQKYYCRVR, CLPKEEQIGKCSTRGRKCCRRKKEAAAK, ASSTTQYA, YTVYGDKIQGKAAYDVSQEVRKYAAYA, ASSTHRKAAYKYIEGNKT, YRLKTLD, AYKLNDDTQVY, YLANKENVHW, NTLSERAAYTTYMDT, YMYYAKRML, QVSDHKNVGP, NFYIRQNHGCN, |
| **Exposed Surface** | KEEQIGK, RKCCRRKKEAAAK, SQEVRKY, HRKAAYKYIEGNK, KLNDDTQ, |
| **Turn** | KLNDDTQ, RQNHGCNI, AAAHHHHHH |
| **Polarity** | KYYCRVRGGRC, SCLPKEEQIGKCSTRGRKCCRRKKEAAAK, VSQEVRKYAA, ASSTHRKAAYKYIEGNK, ANKENVHWA, GAAAHHHHHH |
| **Antigenic Property** | TLQKYYCRVRG, CAVLSCLPKE, YDVSQEV, CIRISMVISLLSMI, TWLIDYV, IVFVFILT, IFLQVSDH, HGCNITV |

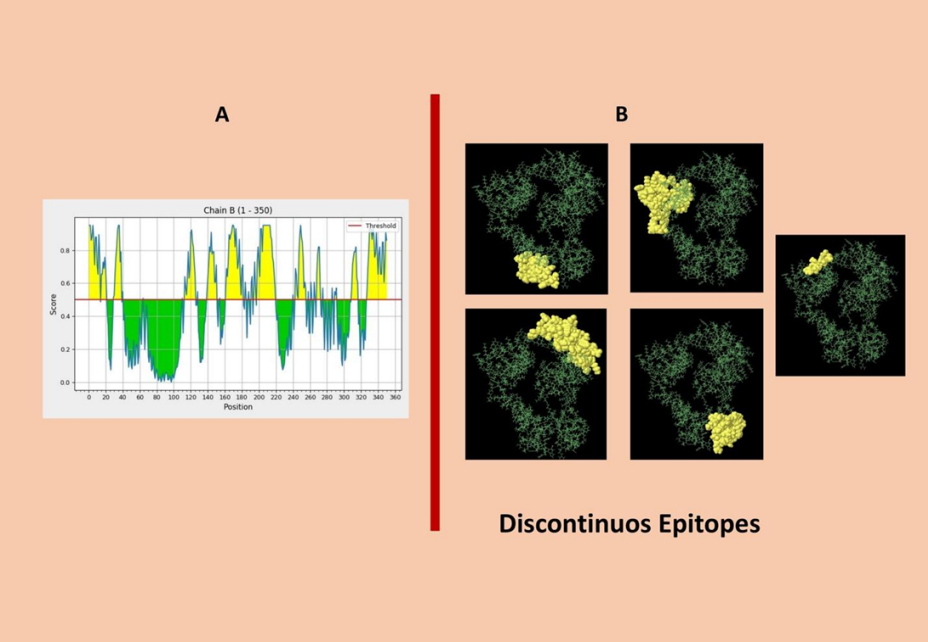


**Figure 6.** (A) 2D plot of the position of discontinuous B-cell epitopes. (B) The 5 predicted discontinuous B-cell epitopes using the Ellipro tool of the IEDB database that the results score were between 0.63-0.77 and the number of residues between 6-49. (Yellow residues: Conformational B-cell epitopes)

server to assess the biophysical stability and variations of the TLR3-vaccine complex. The result of iMODs is demonstrated in **Figure 8**. The variations in the atomic location seen in **Figure 8A** were reflected by the B-factor. The eigenvalue presented in **Figure 8B** represents the stability of the TLR3-vaccine complex. The TLR3-vaccine complex has an eigenvalue of 2.798282e-05, which suggests that the structure is stable and that less energy is needed to distort it. Peaks on the deformability chart, observed in **Figure 8C**, denoted the complex's non-rigid part. The relationship between variance and eigenvalue is inverse. Individual variance is depicted in **Figure 8D** in red, whereas cumulative variance is shown in green. Each dot in the graph denotes one spring between the matching pair of atoms, which is represented by an elastic network graph. Stiffer springs are shown by a darker gray color in Figure 8E of the graph. The covariance map demonstrated the relationship between pairs of residues, as illustrated in **Figure 8E**, where the red, blue, and white colors represent correlated, anti-correlated, and uncorrelated pairs of residues.

## Molecular dynamics simulation

MD simulation is important in forecasting the stability of complex, flexibility, and compactness

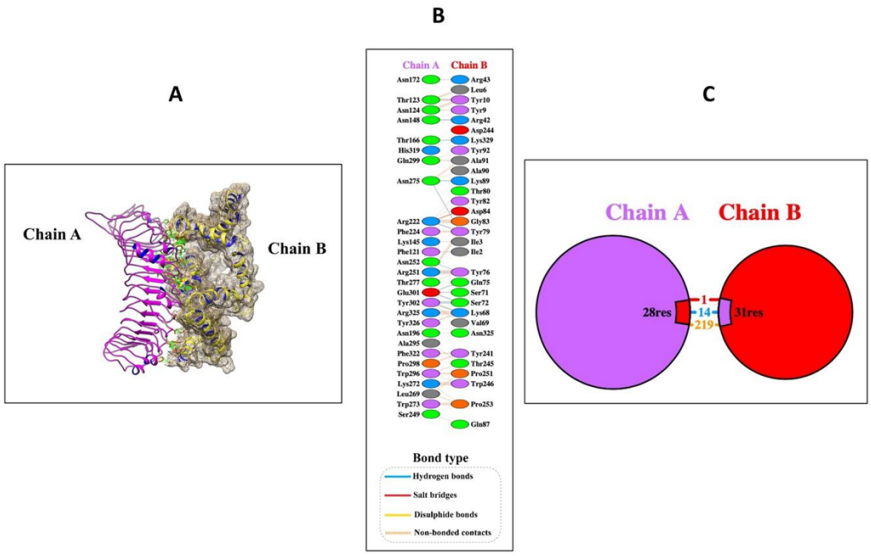


**Figure 7.** (A) Molecular docking between Vaccine and TLR3 (B) The interaction of chain A and chain B and the residues of vaccine and TLR was shown. (C) Several residues that made interaction such as bridge salt, hydrogen bond, and non-bonded contact.

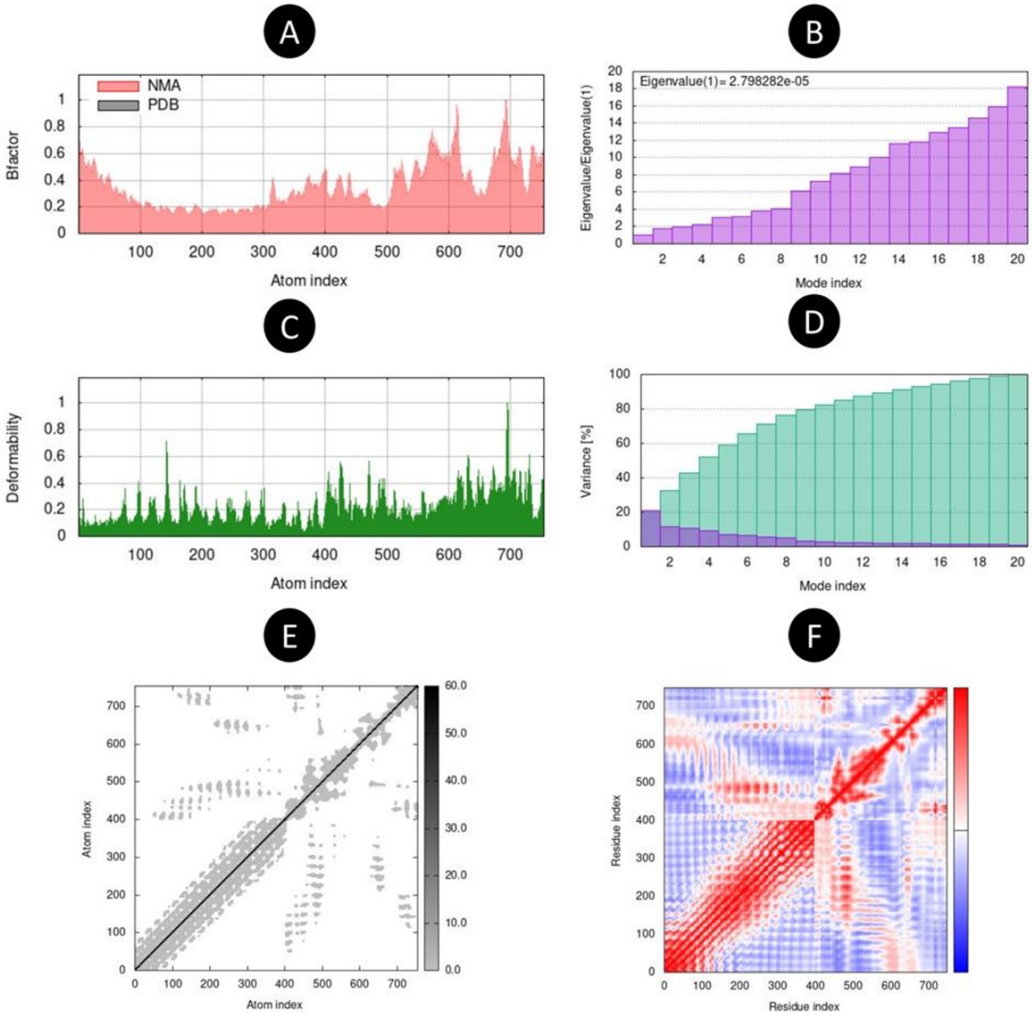


**Figure 8.** Norm mode analysis of TLR3-vaccine complex. (A) B-factor (B), Eigenvalue plot (C), Deformability (D), Variance plot. The red color indicates individual variance, and the green color shows the cumulative (E) Elastic network plot. The dark color indicates the rigid regions (F) in the Co-Variance plot. The red color indicates correlated; blue indicates anti-correlated; and white indicates uncorrelated

that is carried out by GROMACs. The TLR3 and vaccine complex were simulated, and the results were analyzed by graphing data for RMSD, RMSF, and Radius of gyration (Rg). The minimization and two steps equilibration (NVT, NPT) of the system and complex were done as shown in **Figure S2**.

## Stability Analysis

The assessment of structural stability is executed by RMSD graph **(Figure 9)**. After 30 nano - seconds the complex started to become a stable structure. The RMSD plot predicted average, standard deviation (SD), and variance values of about 0.455 nm, 0.070, and 0.004, respectively. The TLR3-vaccine complex supports structural stability and strong binding to TLR3.

## Root-mean Square Fluctuation

Calculation of RMSF can help to estimate the total flexibility of each atom of the TLR3-vaccine complex that is computed. In addition, the RMSF of each atom showed stable fluctuation that RMSF profiles of the TLR3-vaccine complex indicated that most of the atoms had average RMSF profiles of about 0.2 nm, and the larger changes were only for a few atoms. The detailed information was demonstrated in **Figure 9**.

## Radius of Gyration

The radius of gyration (Rg) is frequently used to evaluate a protein's compactness in molecular dynamics simulations of proteins. At the initial time, the radius of gyration increased and then decreased from 20 ns and after 25 ns get stable

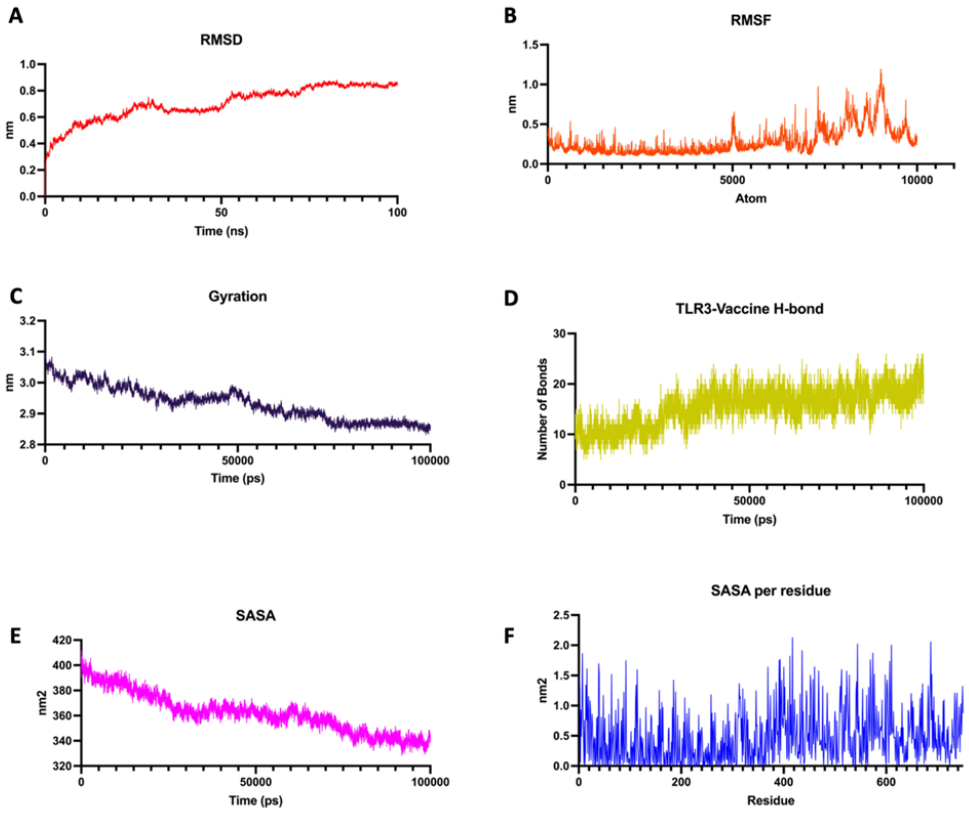


**Figure 9.** Molecular dynamics simulation. (A) Root-mean-square deviation (RMSD), (B) Root-mean-square fluctuation (RMSF), (C) Gyration, (D) TLR3-Vaccine H-bond, (E) SASA, (F) SASA per residue

until 100 ns. The average changes of the Rg are about 2.99 nm with 0.033 SD. The result showed the stability and stiffness of complex. Also, free energy landscape analysis has been calculated and presented. The graph shows energies ranging from -13.2 to 0 KJ **(Figure 9b)**.

## MM/GBSA Calculation

The calculation of binding free energy of the complex (TLR3-vaccine) was calculated and the

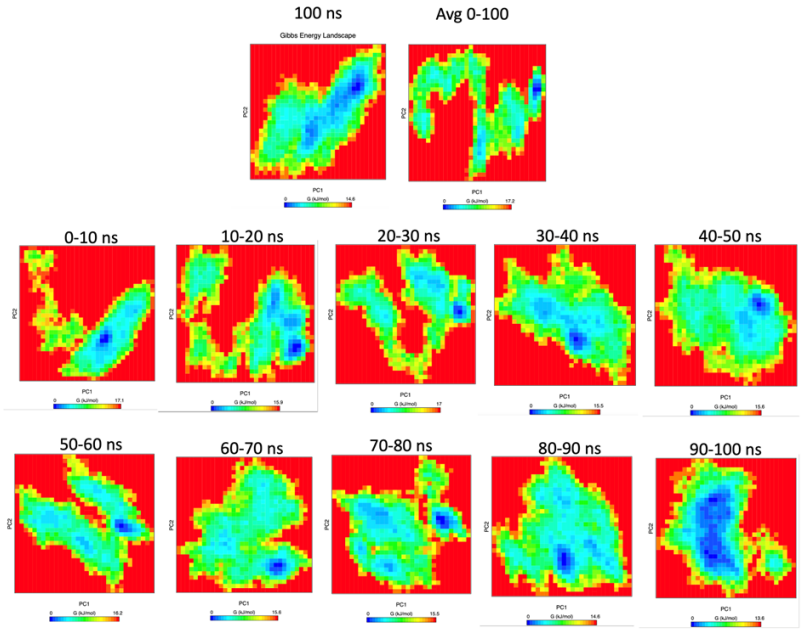


**Figure 9b.** Free energy landscape analysis of molecular dynamics simulation

MM/GBSA method was used before MD simulation and after 10 ns as shown in **Table 5**. The total energy binding before simulation was -20.93 kcal/mol, and then after a 10 ns simulation, -55.1 kcal/mol. Although both complexes are predicted to have negative binding energies, the docked structure is highly affine and conformationally stable. The findings also suggest that the contribution of negative electrostatic energy aids in the generation of negative binding energy.

## Codon Optimization and mRNA Construction

The JCAT online server was performed to do reverse translation and made mRNA that length of mRNA vaccine 1062 nucleotides to sufficient expression in human cells. The CAI value was forecast to be 0.95 that are acceptable and significant. The mean GC content percentage of optimized construct was 67.71% the optimal percentage of GC content requires to be around 30-70% which in this case is the expression of mRNA efficiently in host cells. To design of the mRNA vaccine used different sequences to express in Human host cells sequences including 5ˈ m7GCap-5'UTR-Signal peptide-Start Codon-Multi-epitope vaccine (Open reading frames)-Stop codon-3' UTR-Poly(A) tail that showed in Figure 10A that the final mRNA vaccine consists of 1340 nucleotides. In addition, for the prediction of mRNA structure used the mfold server that showed the secondary structure of the mRNA vaccine **(Figure 10)** and the free energy for the whole mRNA construct was anticipated by the server. The least free energy of the secondary mRNA structure was selected, and the ΔG=-537.80 kcal/mol, and other structural elements were in supplementary data.

## Immune Simulation

For immune response stimulation, we used 3 injections of the MPXV vaccine **(Figure 11)**. The levels of IgM were raised in comparison with IgG. Interestingly, the immunological feedbacks after

**Table5.** Binding free energy of multi-epitope-TLR3 using the MMGBSA method

| Energy components (kcal/mol) | TLR3-vaccine complex | |
|---|---|---|
| | Before MD simulation | After MD simulation (100 ns) |
| Delta G (ΔG) | -20.93 | -55.1 |
| Van der Wall energy | -148.83 | -143.3 |
| Electrostatic energy | 129.74 | -116.64 |
| Electrostatic solvation energy | 17.73 | 222.98 |
| Non-electrostatic solvation energy | -19.57 | -18.14 |

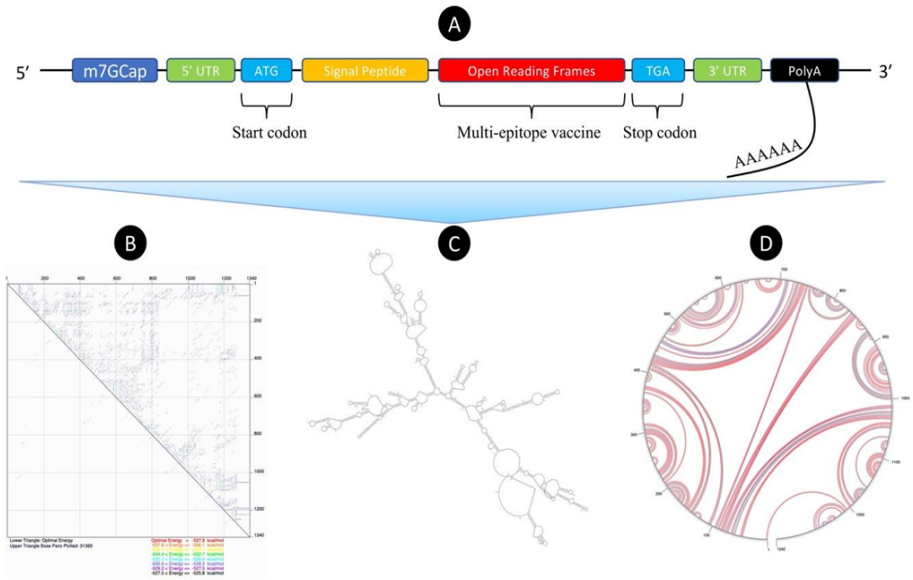


**Figure 10.** The construction of mRNA vaccine based on multi-epitope against MPXV that adapted to human cells for optimal translation. RMSD, RMSF, gyration and SASA are analyzed for the TLR3-vaccine complex. H-bonds between TLR3 and vaccine are also analyzed for the 100-ns trajectory. (A) Parts of the sequence (B) Energy map (C) structural map (D) connectivity map of the predicted RNA.

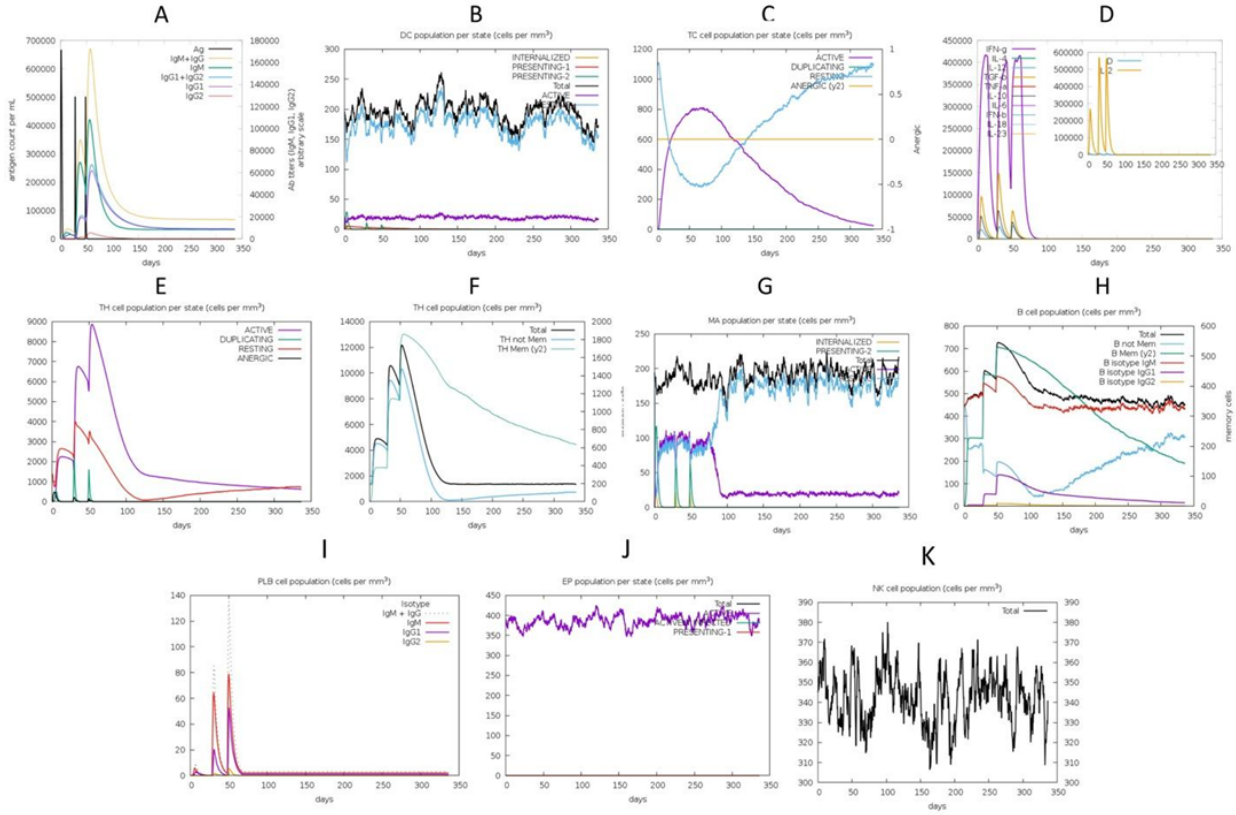


**Figure 11.** Immune simulation: (A) Immunoglobulins and antigens. Antibodies are classified according to their isotype. (B) Dendritic cells. MHC class-I and class-II molecules can both be exposed to antigenic peptides by DC. The curves display the overall number divided into the categories of active, resting, internalized, and displaying the ag. (C) CD8+ T-cytotoxic lymphocytes count per entity-state. (D) Cytokines. The inset plot's high level of cytokines and interleukin D is a warning indicator. (E) CD4+ T-helper lymphocytes count subdivided per entity-state (i.e., active, resting, anergic, and duplicating). (F) CD4 T-helper lymphocytes count. The plot shows total and memory counts. (G) Macrophages. Total count, internalized, presenting on MHC class-II, active and resting macrophages. (H) Each entity-state's B lymphocyte population is represented by counts for active cells, class-II-presenting cells, internalized Ag, duplicated cells, and anergic cells. (I) Each isotype of plasma B cells (IgM, IgG1, and IgG2) is counted separately. (J) Epithelial tissues. The total count is divided into active, virus-infected, and class-I MHC molecule-presenting cells. (K) Natural Killer cells (total count).

second as well as the third dose were suggested to be more prominant than the first immune response. When the antigen was decreased, the concentration of immunoglobulin was stabilized. The mentioned raise could indicate training and that the antigen encounter led to the generation of immune memory; this could indicate trained immunity. An increase in the counts of memory B-lymphocytes following three dosages and the other B isotype we observed were found to be substantial humoral feedback during the time. The B-lymphocytes population activity was discovered as well as the proliferation of B-lymphocytes is raised. Additionally, the CTL/HTL with memory (mem) cells and the macrophage activity was enhanced in that the dendritic cell (DCs) response was present for the three dosages of vaccine, and the total population differed in intensity, ranging from 100 to 250 per $mm^3$. At the end of the immune simulation study, there were enhanced amounts of IFNγ, TGF-β, and IL-10 in the levels of cytokines.

**Analysis of Population Coverage**

For a wide range of alleles, we evaluated the global population coverage for 18 epitopes using the Immune Epitope Database (IEDB) population coverage server. The analysis of worldwide population coverage indicated major heterogeneity in the efficacy and availability of vaccines based on region. The global coverage was favorable. Also, an average regional coverage of 73.96% and a deviation of 20.39% were reported. This suggested considerable differences in population representation, modulated by both genetic diversity and differing allele frequencies in various populations.

European and North American areas indicated an almost complete maximum coverage highlighting the potential capacity of the vaccine to be utilized in continental regions of similar genetic composition. Of note, these regions also showed the highest average hit rates (25.61% and 23.49% respectively) and pc90c (17.19%, 16.15%), in line with strong immunological activation as well as high probability of population-wide efficiency. Moreover, Central America scored the lowest, covering only 7.78% with an average hit of 0.47% and pc90c of 0.43%. It is suggested that future studies attempt to capture a wider range of the population, even though our designed protein proved to be effective based on computational predictions, in most subpopulations. These numbers uncovered an obvious heterogeneity in vaccine efficiency, possibly stemming from varied allelic rates or an underrepresentation of Central American genetic profiles in the pipeline of developing the in silico MPXV immunotherapy. In Northeast Asia, the mean rate of covered population was 61.88% with a hit of 5.08% and pc90c 1.05% which are rather favorable. There is heterogenous coverage in Africa with West Africa improving to 81.33% and Central Africa reporting 65.92% coverage. West Africa exhibits enhanced immunological activation potential (8.52% mean hit, 2.14% pc90c) in spite of similar moderate mean hit rates and pc90c values (8.52%, 2.14%). In Asian areas, coverage is heterogeneous, with East Asia exhibiting an above-average coverage of 78.16%, accompanied by a moderate average hit and pc90c. In a similar fashion, good coverage trends were calculated for South Asia as well as Southeast Asia (71.43%, 66.66%), yet, lower measured levels of immune activation metrics suggest the importance of improving vaccine engineering to specific alleles within populations within these areas. The MPXV vaccine offers better coverage in the West Indies compared to others, with a striking coverage of87.78% and average immunological activation statistics (9.75% hit, 3.27% pc90c), indicating good applicability of the vaccine to this subpopulation. In that regard, Oceania achieves a substantial scoring 78.04% coverage representative of efficient vaccines. Overall, our results may indicate both the success of the vaccine, which achieved broad coverage in the population, but also areas in need of further optimization and specialized candidates targeted to special populations. MPXV targeting approach via designing an immunogenic candidates needs to be adapted to certain regions of the globe where, even though a great bonus in Europe or North America, obtaining comprehensive coverage, Central America, Southeast Asia, and areas of Africa with reduced coverage and baseline immunological activation demand a different approach in order to achieve worldwide coverage **(Figure 12)**.

**MHC Cluster Analysis**

The analysis of MHC I and II was performed by the MHC cluster server that showed the relation

of corresponding MHC I /II alleles that demonstrated the heat map and phylogenetic trees in **Figure S3**.

## Discussion

Monkeypox virus is the newest virus to spread after the COVID-19 pandemic that spread all over the world. In addition, we have not had an extreme pandemic like SARS-CoV-2; therefore, it might be harmful in the future. The effectiveness of vaccines could change when mutations occur at the population level (56,57). The development of reverse vaccinology, immunoinformatic, and proteomics data aids in designing potential and efficient vaccines (58). While it is a relatively new technology, the mRNA approach to vaccine design has drawn significant interest in recent years due to its numerous advantages over traditional vaccine methods. They are not made from live viruses, nor do they contain common additives that come with risks. Some mRNA vaccines have the ability to influence multiple pathogens (viruses and even non-infectious etiologies such as cancer) and mount strong immunological responses for versatile immunoprotection. The multi-epitope mRNA vaccine in this project seeks to provide immunoprotection across related viruses (59,60). The mechanism of the engineered mRNA vaccine is briefly illustrated in **Figure 13**.

Even though the two candidates employ different mechanisms of action, ACAM2000 and JYNNEOS vaccines both have proved to be efficacious against MPXV (61). Recent research has suggested that a single dosage of the JUNNEOS vaccine provides solid immunoprotection against MPTXV infection. Considering a computed efficiency of 78.23% against MPX, the immunogenic candidate could be a valuable prophylactic approach to halt the dissemination of MPXV (62). During pre-clinical studies, several multivalent mRNA-based MPXV vaccines have been developed and researched, namely a quadrivalent (BNT166a) that encodes the A35, B6, M1, and H3 MPXV antigens or a trivalent vac-

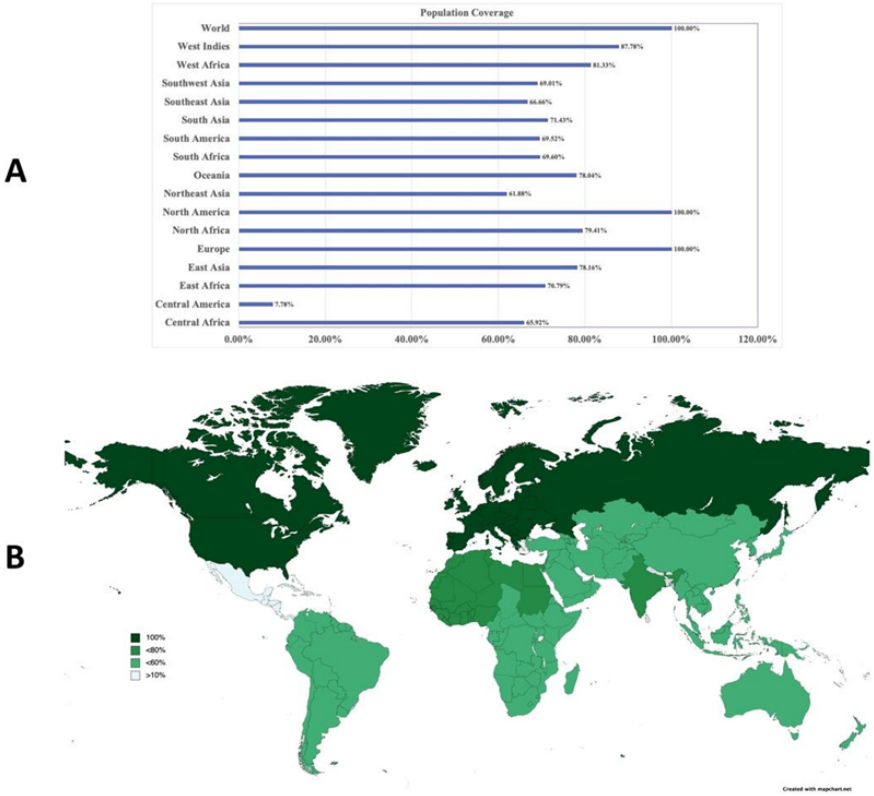


**Figure 12.** (A) Global Population coverage in different locations that showed the highest coverage in the world (B) World map that showed the population coverage (The dark green with the highest population coverage and the light one with the lowest population coverage).

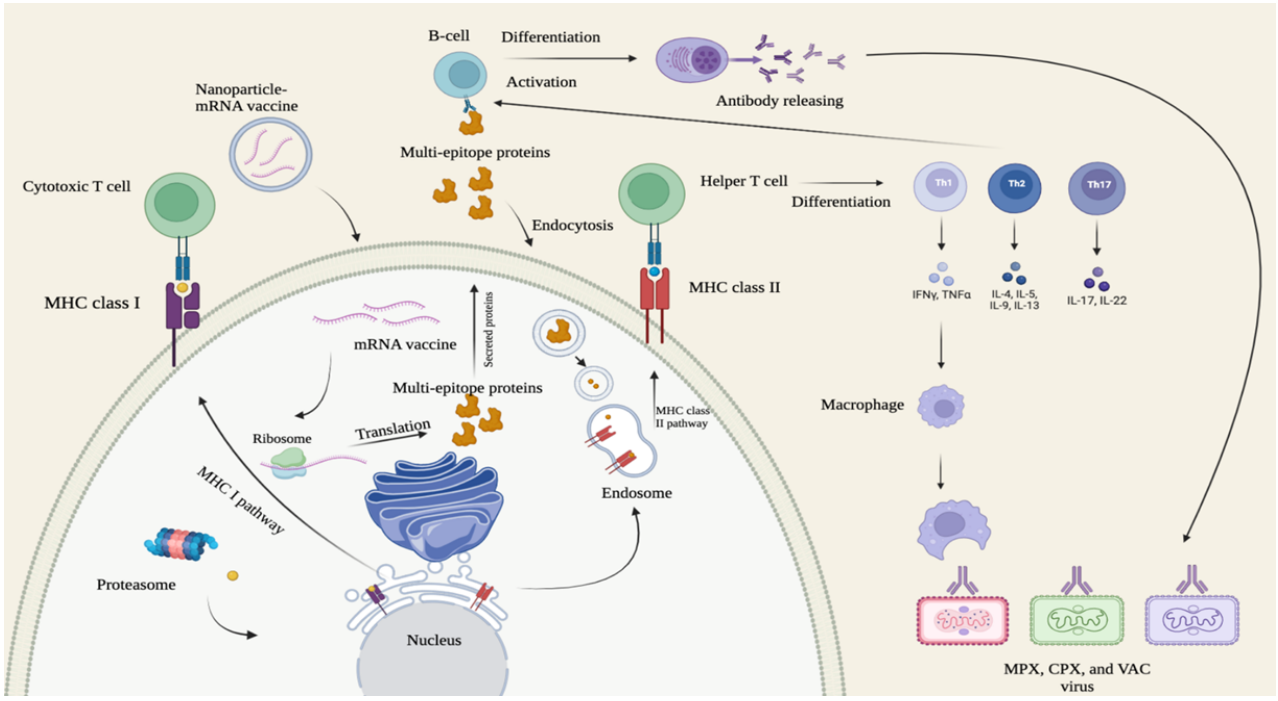


**Figure 13.** The mechanism of mRNA vaccine pathway in the host cell to respond to the B lymphocyte and T lymphocyte. MHC I/II and T Cytotoxic/ T Helper cell pathway.
The antigenic protein synthesized within the cytoplasm is broken down into smaller fragments by proteasomes. These fragments are then transported into the endoplasmic reticulum, where they are loaded onto major histocompatibility complex class I (MHC-I) molecules. MHC-I molecules loaded with the antigen fragments are transported to the cell surface, where they present the antigen to CD8+ T cells. This interaction activates CD8+ T cells, triggering their proliferation and differentiation into cytotoxic T lymphocytes (CTLs). In parallel, antigen-presenting cells (APCs) can also present antigen fragments on major histocompatibility complex class II (MHC-II) molecules. CD4+ T helper cells interact with the antigen-MHC-II complex, leading to their activation and differentiation into various subtypes, such as Th1, Th2, or Th17 cells. Activated T helper cells release cytokines that orchestrate the immune response. Th1 cells, in particular, release IFNγ, stimulating macrophages to enhance their phagocytic and bactericidal activities. Th2 cells promote antibody production by B cells, leading to the generation of a robust humoral response. B cells recognize the antigen through their surface immunoglobulin receptors and receive help from Th2 cells. This interaction triggers B cell activation, leading to proliferation, differentiation into plasma cells, and secretion of antigen-specific antibodies. Antibodies generated in response to the mRNA vaccine bind to the target antigen, neutralizing pathogens, preventing their entry into cells, and facilitating their clearance by other components of the immune system, such as complement proteins and phagocytes. Adapted from and Created with BioRender.com

cine (BNT166c) that does not employ the H3 antigen. Both vaccines have been shown to elicit activation of dominant T-lymphocyte responses and IgG Abs (346, 356, 365) as well as neutralizing antibodies for MPXV and vaccinia virus (357, 365). In addition, BNT166a/BNT166c demonstrated strong immunoprotection towards vaccinia virus and class-I as well as class-IIb MPXV. It is worth highlighting that the BNT166a vaccination presented an extraordinary efficacy in the prevention of death. The data in this study indicate that multivalent mRNA immunotherapies may potentially elicit strong immunological responses (63). The mRNA-based method of immunotherapy development was found to induce a much more powerful immunological response than the biological agents from the early immunotherapies and against conventional immunization methods in many instances. It is crucial to note that mRNA-based immunotherapies have their special challenges as well. The COVID-19 mRNA immune-modulating curatives have been associated with certain adverse events, such as local injection site reactions, fever, or fatigue, and in a few patients, severe reactions such as myocarditis or anaphylaxis have been reported. Even though these adverse reactions are primarily transient and can often be successfully treated in nature, current evidence highlights the importance of extensive safety evaluations for any

new mRNA-reliant immunomodulatory candidates. Furthermore, the potential of deleterious sequelae in certain subpopulations also calls for the necessary degree of caution in maintaining any clinical studies into future generations of all the experiments, especially for an immunotherapy that is aimed at a much wider demographic spectrum (64).

The present work employs immunoinformatic approaches to engineer a suitable mRNA vaccine that can stimulate a potent immunological response targeting MPXV, cowpox, and vaccinia viruses. The MPXV possesses multiple surface proteins that need to be examined for designing the advanced mRNA vaccine to prevent the infection. The first step consists of the identification of immunogenic antigens and is the most crucial part of the engineering of the multi-peptide that will undergo reverse transcription into an mRNA vaccine. The three antigens (i.e. A35R, cell surface binding and M1R) using the probable antigen to design a vaccine against MPXV and those antigens are conserved in Cowpox and Vaccinia virus to design the trivalent mRNA vaccine (65). An experiment recently designed a multi-epitope immunotherapy targeting A30L, A35R, A29L, L1R, M1R, and E8L. The present experiment attempted to target A35R, cell surface-attaching proteins, and M1R (66). Of note is that the proposed vaccination is a trivalent offering with various benefits. As suggested by our preliminary data, this novel in silico MPXV immunotherapy can provoke broad and robust immunological responses. The present strategy targeted three MPXV antigens. Preclinical screening of related mRNA immunogenic candidates, particularly BNT166a/c, has demonstrated the potential to induce T-lymphocyte feedbacks, raise IgG Ab levels, in addition to mounting neutralizing activity against either MPXV or similar orthopoxviruses. It is notable that BNT166g induced strong immunoprotection towards lethal viral challenges, highlighting the potency of mRNA immunogenic options.

After that, we selected the most immunogenic epitopes that can be used to generate an efficient vaccine from the IEDB server. To create the final vaccine, we connected the anticipated immunogenic epitopes from A35R, Cell surface binding, and M1R using various linkers such as EAAAK, GGGS, GPGPG, and AAY. This multi-peptide construct can induce a broad immune response against the target viruses (67). An important aspect of this study was the analysis of IFNγ and IL-4 epitopes in the multi-epitope vaccine. Including epitopes that induce both humoral and cellular immune systems is crucial for generating a comprehensive immune reaction. IFNγ is key for immunity against viral infections, activating macrophages and inducing MHC II protein production (68,69). Furthermore, the conserved T-lymphocyte epitopes between Monkeypox, Vaccinia, and Cowpox demonstrated the significance of target proteins. The analysis of our designed vaccine demonstrated structural stability, thermal stability, antigenicity probability, and non-allergenicity, which have favorable values for vaccine design.

IL-4 stimulates the proliferation of B cells and T cells and the differentiation of B cells (70,71). To analyze multi-epitope sequences and identify IFNγ and IL-4 inducers, we used the IFNepitope server with an SVM algorithm. The prediction of secondary and tertiary structures of the multi-epitope vaccine, along with their validation, provided valuable insights into the stability and antigenic properties of the vaccine. Understanding the structural characteristics of the vaccine is crucial for its proper folding, stability, and recognition by the immune system. We utilized the online server to estimate the secondary and tertiary structure and quality of the 3D structure of the multi-epitope vaccine (25,72). Analysis of the integrity of our engineered vaccine construct using protein quality assessment tools (ERRAT, PROCHECK, and Ramachandran analysis) corroborated its construct integrity, indicating that 92.3% of amino acids were localized to most allowed areas. Implementation of disulfide bond design enhanced the stability of the MPXV vaccine, and the Z-score displayed an enhanced construct quality with a more favorable Z-score value which was improved from 6.02 to 6.25.

The engineering of disulfide bonds in the vaccine is a strength of this study. Disulfide bonds play a quintessential function in maintaining the structural integrity of proteins. Through engineering disulfide bonds, we enhanced the stability of the vaccine, antigenicity, as well as resistance to proteolytic degradation (73). We highlight the significance of predicting linear and conformational

B lymphocyte cell epitopes in the multi-epitope vaccine for which the score was between 0.77 and 0.64. These epitopes can interact with antibodies, inducing the production of neutralizing antibodies essential for virus clearance or neutralization.

For the interactions of TLR3 and the designed vaccine, molecular docking was conducted. Since TLR3 perceives viral components and amplifies immune responses, this assessment offered insight into the strength of binding (−352.51). Additionally, predicted one salt Bridge and 14 H-bonded interactions for the interface of the vaccine and the TLR3 complex. Such observation provides important data concerning, not only the TLR3 receptor (a leading innate immune molecule selectively activated by vaccines) but also the molecular interaction registered between the engineered vaccine and TLR3 (74,75).

The docked complex containing the stabilized vaccine structure and TLR3, was moved onto the molecular dynamics simulation phase. With advancements in computational resources and improved all-atom force fields, MDS provides a valuable tool to predict the conformational evolution of systems governed by Newtonian molecular mechanics. The all-atom forcefield-based approach was chosen for simulating the MPXV vaccine-TLR3 complex. The vaccine-TLR3 complex was analyzed for the flexibility of protein regions, surface accessibility to solvents, and binding energies (76). The binding free energy (ΔG) calculation indicated that energy was reduced from −20.93 to −55.1 Kcal/mol at the end of the simulation, as a result supporting the stable and strong binding of vaccine-TLR3. The van der Waals energies supported stable binding, yielding -148.8 Kcal/mol and -143.3 Kcal/mol at the beginning and end of the simulation, respectively. This indicates that hydrophilic interactions are stable throughout the MD run. Assessment of electrostatic energy showed a value of 129.74 Kcal/mol in the beginning and –116.64 Kcal/mol in the last frame of the MD production run. This is likely due to the way polar interactions either strengthen or disrupt as the conformation of the protein complex adapts to the solvent. The electrostatic solvation energies were 17.73 Kcal/mol and 222.98 Kcal/mol, respectively, potentially reflecting the effect of the solvent in the modulation of the polar regions in the protein complex. Non-electrostatic solvation energies were -19.57 Kcal/mol and -18.14 Kcal/mol, before and after the MDS, respectively. Nevertheless, it still affirms that the TLR3-vaccine complex binds very stably, but the complex was adapting to the solvent (TIP3P water) throughout the MDS.

This made possible a more precise computation of the binding free energy of the vaccine-receptor complex. Analysis of the conformational stability of the TLR3-vaccine complex using the iMODS server was accomplished. This analysis shed light on the relationship between complex dynamic motion and rigidity with the aid of factors such as NMA mobility, Ei-genvalues, B-factor, variance, covariance map, as well as linkage matrix (77).

The reverse translation of the vaccine construct using the JCAT online server showed that production in humans could be accomplished with a total mRNA length of 1062 nucleotides. The CAI value of 0.95, which characterizes efficient translation of the host system, verified this optimization. The GC content of the optimized structure was computed to be 67.71%, which was in the accepted range of 30 to 70%. Complementary to supporting efficient mRNA expression, this balanced GC content may also provide construct stability and reduced degradation risk, as a result, augmenting the translational potential of our MPXV candidate in host cells.

The MPXV mRNA vaccine design was carefully optimized to mimic natural mRNA motifs for optimal stability as well as translational efficiency. We assembled an mRNA consisting of the following key components: a 5◦ m7G cap, 5◦ UTR, a signal peptide, start codon, the multi-epitope immunotherapy open reading frame (ORF), stop codon, 3◦ UTR, and a poly(A) tail. These elements ensure the mRNA's integrity, efficient translation, and immune activation. These components are key for mRNA stability, efficient translation, and immune activation. The resultant construct, 1340 nucleotides long, was optimized for strong expression. This mRNA vaccine has a tertiary structure, as computed by the mfold tool, which shows its thermal dynamic stability. A very low free energy was computed (ΔG = -537.80 Kcal/mol), which is indicative of a highly stable structure, required for translation to proceed fluidly, and reacting via conformational

change with host cellular machinery. This stable secondary structure attenuates the potential for degradation by RNases while simultaneously maintaining the appropriate functional conformation sensed through ribosomes to begin translation. The range of expected mRNA secondary constructs (supplementary material) further deciphered the favorable structural aspects of the built mRNA immunogenic candidate. Furthermore, incorporation of optimised regulatory elements such as the 5◦ UTR and 3◦ UTR is in keeping with mRNA vaccine constructs for other infectious diseases, which are shown to improve stability and translation efficiency. In summary, the low ΔG and the nucleotide optimization indicate the benefit of this design strategy compared to classical immunotherapy constructs. The mRNA vaccine structure developed here presents a careful balance of stability, efficacy, and immunogenicity. Furthermore, the construct and thermodynamic features of the mRNA additionally validate its potential as a potent and efficient target for vaccinology. In vitro and in vivo experiments will need to be done to determine its expression efficiency and immune response. The immune system plays a major role in the course of infection in humans (53,78,79). Bioinformatics studies could help estimate the safety and efficacy as well as rapidly validate immunotherapeutic candidates such as mRNA and protein vaccines, CAR T-cells, T-cell engagers and many other type of immunomodulatory candidates (80,81) Such results indicate that there is good potential in employing computational approaches to accelerate the design of immunogenic candidates (82–84), making way for scalable, safe, as well as effective vaccine development towards new pathogens such as MPX.

The immunostimulatory features of the vaccine were assessed using C-ImmSim. These simulations provide invaluable information on the kinetics of immune cell activation, cytokine production, and the efficacy of the suggested candidate in stimulating an immune reply (85). We performed a population coverage analysis to assess the effectiveness and coverage of the multi-epitope vaccine across diverse populations. In contrast to the previous study, the candidate vaccine has better population coverage (66). By considering the diversity of MHC alleles within each population, we predicted the percentage of individuals who would potentially respond to the vaccine. In the end, we utilized the MHCcluster server to analyze MHC I and MHC II alleles.

This analysis revealed the relationship between corresponding MHC I/II alleles. This information is important for predicting the vaccine efficacy and immunogenicity in various individuals. A significant drawback of our approach was the inability of reverse vaccinology to identify non-protein targets such as polysaccharides. Another limitation of our study was the potential for an extended MDS trajectory. In recent years, multiple immunoinformatics approaches have changed the pipeline for vaccine development, making it possible a cost-efficient and accelerated design of candidates. These pipelines are still speculative. This is because they rely on a limited set of existing known databases , which may not cover the complete complexity of host-pathogen interactions or new circulating variants. The potential to precisely forecast epitopes relies on good input data diversity, and certain immunological features, such as post-translational changes or structural conformations, may be neglected. These forecasts are made via computational approaches that require experimental confirmation. Indeed, it is necessary to confirm all the predicted candidates through rigorous preclinical studies to validate their immunogenicity, safety profile, and efficiency is crucial. As a result, even though Immunoinformatics provides a valuable platform for screening vaccine targets, good quality experimental studies are necessary to follow their results to offer practical safety and efficacy (86,87). Therefore, future experimental studies will be conducted in vitro and in vivo, such as cell lines and animal models, to validate these findings (88). Computational biology could be used to facilitate vaccine design against various disease conditions (89). In times of pandemic and outbreaks such as COVID-19 and MPXV, rapid development of therapeutics and investigation of their immunological underlying is of utmost importance. This process could be facilitated by computational biology approaches (90–93). In addition to pharmaceutical products, a wide range of herbals have been suggested for infectious and non-infectious diseases (94–96). Also, we believe targeting herbals as well as modern medicine products could be facilitated

by Immunoinformatics analyses which could be attempted in the future. By pursuing these future directions, the project can contribute to the development of a potent mRNA vaccine with broad protection against monkeypox, cowpox, and vaccinia viruses. Clues from the present study could address the medical need for effective vaccines against these viral infections and make a considerable influence on public health. Additionally, we believe using Immunoinformatics in the outbreak era of MPX is especially useful as rapid design of candidates is very crucial to slow the progress of the infection and mortality rates. Bioinformatics-assisted vaccine design makes possible the rapid design of such candidates. Further wet lab experimentation to validate vaccine in the present study is highly suggested.

## Conclusion

The main aim of this study was to provide initial computational clues on the engineering of a new mRNA vaccine employing a multi-epitope strategy to stimulate humoral and cell-regulated immunity targeting MPXV. Immunogenic epitopes extarcted from three of the key proteins of MPXV, namely cell surface binding protein, A35R and M1R was accomplished using computational Immunoinformatics approaches. The selected proteins have high immunogenic potential and could as a result be effective aims for immunotherapy design. The investigation portrays the generation of a novel trivalent mRNA vaccine, that especially targets the previously identified epitopes from the MPXV as well as the conserved epitopes shared with CPXV and VACV. This special architecture broadens immunological reactions and is believed to deliver immunoprotection and protects against a variety of Orthopoxvirus infections. Using conserved areas common to these related viruses, the immunotherapy could display robust immunological responses, enhancing protection from MPXV, CPXV, and VACV infections. This effort is a key advancement in the development of mRNA vaccines building on computational efforts to forecast and validate immunogenic epitopes in an mRNA based immunotherapy which could be utilized to address Orthopoxvirus outbreaks. This versatile design of the trivalent mRNA vaccine is capable of inducing protective immunity by simultaneously targeting multiple viral proteins with cell surface receptor binding, A35R, and M1R proteins to act as immunological targets. Further experimental validation of this approach and the candidate vaccine will be needed to understand its efficacy. We believe the present study could provide a valuable pipeline for rapid design of immunogenic candidates. Further wet lab study is warranted.

## Conflict of Interest

The authors declare no competing interests.

## References


1. Alakunle E, Moens U, Nchinda G, Okeke MI. Monkeypox Virus in Nigeria: Infection Biology, Epidemiology, and Evolution. Viruses. 2020;12(11).
2. Shchelkunov SN, Totmenin A V, Safronov PF, Mikheev M V, Gutorov V V, Ryazankina OI, et al. Analysis of the monkeypox virus genome. Virology. 2002 Jun;297(2):172–94.
3. Cho CT, Wenner HA. Monkeypox virus. Bacteriol Rev. 1973 Mar;37(1):1–18.
4. Marennikova SS, Moyer RW. Classification of Poxviruses and Brief Characterization of the Genus Orthopoxvirus. In: Orthopoxviruses Pathogenic for Humans. Boston, MA: Springer US; 2005. p. 11–8.
5. Bunge EM, Hoet B, Chen L, Lienert F, Weidenthaler H, Baer LR, et al. The changing epidemiology of human monkeypox-A potential threat? A systematic review. PLoS Negl Trop Dis. 2022 Feb;16(2):e0010141.
6. Kozlov M. Monkeypox outbreaks: 4 key questions researchers have. Vol. 606, Nature. England; 2022. p. 238–9.
7. Vogel L. Making sense of monkeypox death rates. CMAJ. 2022 Aug;194(31):E1097.
8. Muniandy T, Abdullah N. Monkeypox: A Comprehensive Review. International Journal of Online Pedagogy and Course Design. 2022;13(1):1–15.
9. Schmidt FI, Bleck CKE, Mercer J. Poxvirus host cell entry. Curr Opin Virol. 2012;2(1):20–7.
10. Banuet-Martinez M, Yang Y, Jafari B, Kaur A, Butt ZA, Chen HH, et al. Monkeypox: a review of epidemiological modelling studies and how modelling has led to mechanistic insight. Epidemiol Infect. 2023 May;151:e121.
11. Zovi A, Ferrara F, Langella R, Vitiello A. Pharmacological Agents with Antiviral Activity against Monkeypox Infection. Int J Mol Sci. 2022 Dec;23(24).
12. Hooper JW, Custer DM, Schmaljohn CS, Schmaljohn AL. DNA vaccination with vaccinia virus L1R and A33R genes protects mice against a lethal poxvirus challenge. Virology. 2000 Jan;266(2):329–39.
13. Hou F, Zhang Y, Liu X, Murad Y, Xu J, Yu Z, et al. Novel mRNA vaccines encoding Monkeypox virus M1R and A35R protect mice from a lethal virus challenge. bioRxiv. 2022;
14. Sagdat K, Batyrkhan A, Kanayeva D. Exploring monkeypox virus proteins and rapid detection techniques. Front Cell Infect Microbiol. 2024;14:1414224.
15. Saleki K, Mohamadi MH, Alijanizadeh P, Rezaei N.

Neurological adverse effects of chimeric antigen receptor T-cell therapy. Expert Rev Clin Immunol. 2023;19(11):1361–83.
16. Mohseni Afshar Z, Babazadeh A, Janbakhsh A, Afsharian M, Saleki K, Barary M, et al. Vaccine-induced immune thrombotic thrombocytopenia after vaccination against Covid-19: a clinical dilemma for clinicians and patients. Rev Med Virol. 2022;32(2):e2273.
17. Saleki K, Payandeh P, Shakeri M, Pourahmad R, Banazadeh M, Alijanizadeh P, et al. Utilizing immunoinformatics to target brain tumors; an aid to current neurosurgical practice. Interventional Pain Medicine and Neuromodulation. 2022;2(1).
18. Khan S, Khan A, Rehman AU, Ahmad I, Ullah S, Khan AA, et al. Immunoinformatics and structural vaccinology driven prediction of multi-epitope vaccine against Mayaro virus and validation through in-silico expression. Infect Genet Evol. 2019 Sep;73:390–400.
19. Omoniyi AA, Adebisi SS, Musa SA, Nzalak JO, Danborno B, Bauchi ZM, et al. Designing a multi-epitope vaccine against the Lassa virus through reverse vaccinology, subtractive proteomics, and immunoinformatics approaches. Inform Med Unlocked. 2021;25:100683.
20. Rao AK, Petersen BW, Whitehill F, Razeq JH, Isaacs SN, Merchlinsky MJ, et al. Use of JYNNEOS (Smallpox and Monkeypox Vaccine, Live, Nonreplicating) for Preexposure Vaccination of Persons at Risk for Occupational Exposure to Orthopoxviruses: Recommendations of the Advisory Committee on Immunization Practices - United States, 2022. MMWR Morb Mortal Wkly Rep. 2022 Jun;71(22):734–42.
21. Babkin I V, Babkina IN, Tikunova N V. An Update of Orthopoxvirus Molecular Evolution. Viruses. 2022 Feb;14(2).
22. Home M, Populations S. Interim Clinical Considerations for Use of JYNNEOS and ACAM2000 Vaccines during the 2022 U.S. Mpox Outbreak | Mpox | Poxvirus | CDC. 2023;(Cdc):28–30.
23. Goel RR, Painter MM, Apostolidis SA, Mathew D, Meng W, Rosenfeld AM, et al. mRNA vaccines induce durable immune memory to SARS-CoV-2 and variants of concern. Science (1979). 2021;374(6572):abm0829.
24. Al Tbeishat H. Novel In Silico mRNA vaccine design exploiting proteins of M. tuberculosis that modulates host immune responses by inducing epigenetic modifications. Sci Rep. 2022 Mar;12(1):4645.
25. Saleki K, Alijanizade P, Moradi S, Rahmani A, Banazadeh M, Mohamadi MH, et al. Engineering a novel immunogenic chimera protein utilizing bacterial infections associated with atherosclerosis to induce a deviation in adaptive immune responses via Immunoinformatics approaches. Infect Genet Evol. 2022 Aug;102:105290.
26. Aziz S, Almajhdi FN, Waqas M, Ullah I, Salim MA, Khan NA, et al. Contriving multi-epitope vaccine ensemble for monkeypox disease using an immunoinformatics approach. Front Immunol. 2022;13.
27. Yousaf M, Ismail S, Ullah A, Bibi S. Immuno-informatics profiling of monkeypox virus cell surface binding protein for designing a next generation multi-valent peptide-based vaccine. Front Immunol. 2022;13:1035924.
28. Pardi N, Hogan MJ, Weissman D. Recent advances in mRNA vaccine technology. Curr Opin Immunol. 2020;65:14–20.
29. Oluwagbemi OO, Oladipo EK, Kolawole OM, Oloke JK, Adelusi TI, Irewolede BA, et al. Bioinformatics, Computational Informatics, and Modeling Approaches to the Design of mRNA COVID-19 Vaccine Candidates. Computation. 2022;10(7).
30. Linares-Fernández S, Lacroix C, Exposito JY, Verrier B. Tailoring mRNA Vaccine to Balance Innate/Adaptive Immune Response. Trends Mol Med. 2020;26(3):311–23.
31. Dhople V, Krukemeyer A, Ramamoorthy A. The human beta-defensin-3, an antibacterial peptide with multiple biological functions. Biochim Biophys Acta. 2006 Sep;1758(9):1499–512.
32. Ferris LK, Mburu YK, Mathers AR, Fluharty ER, Larregina AT, Ferris RL, et al. Human beta-defensin 3 induces maturation of human langerhans cell-like dendritic cells: an antimicrobial peptide that functions as an endogenous adjuvant. J Invest Dermatol. 2013 Feb;133(2):460–8.
33. Fadaka AO, Sibuyi NRS, Martin DR, Goboza M, Klein A, Madiehe AM, et al. Immunoinformatics design of a novel epitope-based vaccine candidate against dengue virus. Sci Rep. 2021 Oct;11(1):19707.
34. Doytchinova IA, Flower DR. VaxiJen: a server for prediction of protective antigens, tumour antigens and subunit vaccines. BMC Bioinformatics. 2007 Jan;8:4.
35. Gupta S, Kapoor P, Chaudhary K, Gautam A, Kumar R, Raghava GPS. Peptide toxicity prediction. Methods Mol Biol. 2015;1268:143–57.
36. Saha S, Raghava GPS. AlgPred: prediction of allergenic proteins and mapping of IgE epitopes. Nucleic Acids Res. 2006;34(suppl_2):W202–9.
37. Altschul SF, Gish W, Miller W, Myers EW, Lipman DJ. Basic local alignment search tool. J Mol Biol. 1990 Oct;215(3):403–10.
38. Grassegger A, Höpfl R. Significance of the cytokine interferon gamma in clinical dermatology. Clin Exp Dermatol. 2004;29(6):584–8.
39. Tur J, Farrera C, Sánchez-Tilló E, Vico T, Guerrero-Gonzalez P, Fernandez-Elorduy A, et al. Induction of CIITA by IFN-γ in macrophages involves STAT1 activation by JAK and JNK. Immunobiology. 2021;226(5):152114.
40. Park H, Kim DE, Ovchinnikov S, Baker D, DiMaio F. Automatic structure prediction of oligomeric assemblies using Robetta in CASP12. Proteins: Structure, Function, and Bioinformatics. 2018;86:283–91.
41. Saleki K, Alijanizadeh P, Javanmehr N, Rezaei N. The role of Toll-like receptors in neuropsychiatric disorders: Immunopathology, treatment, and management. Med Res Rev. 2024;44(3):1267–325.
42. Saleki K, Mohamadi MH, Banazadeh M, Alijanizadeh P, Javanmehr N, Pourahmad R, et al. In silico design of a TLR4-mediating multiepitope chimeric vaccine against amyotrophic lateral sclerosis via advanced immunoinformatics. J Leukoc Biol. 2022;112(5):1191–207.
43. Yan Y, Zhang D, Zhou P, Li B, Huang SY. HDOCK: a web server for protein–protein and protein–DNA/RNA docking based on a hybrid strategy. Nucleic Acids Res. 2017;45(W1):W365–73.

44. Laskowski RA, Jabłońska J, Pravda L, Vařeková RS, Thornton JM. PDBsum: Structural summaries of PDB entries. Protein Sci. 2018 Jan;27(1):129–34.
45. Saleki K, Aram C, Alijanizadeh P, Khanmirzaei MH, Vaziri Z, Ramzankhah M, et al. Matrix metalloproteinase/Fas ligand (MMP/FasL) interaction dynamics in COVID-19: An in silico study and neuroimmune perspective. Heliyon. 2024 May 30;10(10).
46. Weng G, Wang E, Wang Z, Liu H, Zhu F, Li D, et al. HawkDock: a web server to predict and analyze the protein–protein complex based on computational docking and MM/GBSA. Nucleic Acids Res. 2019;47(W1):W322–30.
47. Grote A, Hiller K, Scheer M, Münch R, Nörtemann B, Hempel DC, et al. JCat: a novel tool to adapt codon usage of a target gene to its potential expression host. Nucleic Acids Res. 2005 Jul;33(Web Server issue):W526-31.
48. Pollard C, De Koker S, Saelens X, Vanham G, Grooten J. Challenges and advances towards the rational design of mRNA vaccines. Trends Mol Med. 2013 Dec;19(12):705–13.
49. Kim SC, Sekhon SS, Shin WR, Ahn G, Cho BK, Ahn JY, et al. Modifications of mRNA vaccine structural elements for improving mRNA stability and translation efficiency. Mol Cell Toxicol. 2022;18(1):1–8.
50. Tcherepanova IY, Adams MD, Feng X, Hinohara A, Horvatinovich J, Calderhead D, et al. Ectopic expression of a truncated CD40L protein from synthetic post-transcriptionally capped RNA in dendritic cells induces high levels of IL-12 secretion. BMC Mol Biol. 2008 Oct;9:90.
51. Kwon H, Kim M, Seo Y, Moon YS, Lee HJ, Lee K, et al. Emergence of synthetic mRNA: In vitro synthesis of mRNA and its applications in regenerative medicine. Biomaterials. 2018 Feb;156:172–93.
52. Thomsen M, Lundegaard C, Buus S, Lund O, Nielsen M. MHCcluster, a method for functional clustering of MHC molecules. Immunogenetics. 2013 Sep;65(9):655–65.
53. Reinke S, Thakur A, Gartlan C, Bezbradica JS, Milicic A. Inflammasome-mediated immunogenicity of clinical and experimental vaccine adjuvants. Vaccines (Basel). 2020;8(3):554.
54. Saleki K, Mohamadi M, Alijanizadeh P, Rezaei N. Inflammasome elements in epilepsy and seizures. In: Translational Neuroimmunology, Volume 7. Elsevier; 2023. p. 449–74.
55. Alizadehmoghaddam S, Pourabdolhossein F, Najafzadehvarzi H, Sarbishegi M, Saleki K, Nouri HR. Crocin attenuates the lipopolysaccharide-induced neuroinflammation via expression of aim2 and nlrp1 inflammasome in an experimental model of parkinson's disease. Heliyon. 2024;10(3).
56. Zhang Y, Zhang JY, Wang FS. Monkeypox outbreak: A novel threat after COVID-19? Mil Med Res. 2022;9(1):29.
57. Atefi A, Ghanaatpisheh A, Ghasemi A, Haghshenas H, Eyvani K, Bakhshi A, et al. Meningitis after COVID-19 vaccination, a systematic review of case reports and case series. BMC Infect Dis. 2024;24(1):1138.
58. Aiman S, Alhamhoom Y, Ali F, Rahman N, Rastrelli L, Khan A, et al. Multi-epitope chimeric vaccine design against emerging Monkeypox virus via reverse vaccinology techniques- a bioinformatics and immunoinformatics approach. Front Immunol. 2022;13.
59. Schlake T, Thess A, Fotin-Mleczek M, Kallen KJ. Developing mRNA-vaccine technologies. RNA Biol. 2012 Nov;9(11):1319–30.
60. Pardi N, Hogan MJ, Porter FW, Weissman D. mRNA vaccines — a new era in vaccinology. Nat Rev Drug Discov. 2018;17(4):261–79.
61. Kandeel M, Morsy MA, Abd El-Lateef HM, Marzok M, El-Beltagi HS, Al Khodair KM, et al. Efficacy of the modified vaccinia Ankara virus vaccine and the replication-competent vaccine ACAM2000 in monkeypox prevention. Int Immunopharmacol. 2023;119:110206.
62. Taha AM, Mahmoud AM, Abouelmagd K, Saed SAA, Khalefa BB, Shah S, et al. Effectiveness of a single dose of JYNNEOS vaccine in real world: A systematic review and meta-analysis. Health Sci Rep. 2024 Sep;7(9):e70069.
63. Zuiani A, Dulberger CL, De Silva NS, Marquette M, Lu YJ, Palowitch GM, et al. A multivalent mRNA monkeypox virus vaccine (BNT166) protects mice and macaques from orthopoxvirus disease. Cell. 2024 Mar;187(6):1363-1373.e12.
64. Gidwani R, Siddiqui S, Prabhavalkar S. REACTIVE NON-REGIONAL LYMPHADENOPATHY FROM THE COVID-19 mRNA VACCINE: A NOVEL SIDE-EFFECT. Vol. 91, The Ulster medical journal. Northern Ireland; 2022. p. 166–7.
65. Yefet R, Friedel N, Tamir H, Polonsky K, Mor M, Hagin D, et al. A35R and H3L are Serological and B Cell Markers for Monkeypox Infection. medRxiv. 2022;
66. Kaur A, Kumar A, Kumari G, Muduli R, Das M, Kundu R, et al. Rational design and computational evaluation of a multi-epitope vaccine for monkeypox virus: Insights into binding stability and immunological memory. Heliyon. 2024;10(16):e36154.
67. Saleki K, Mohamadi MH, Banazadeh M, Alijanizadeh P, Javanmehr N, Pourahmad R, et al. In silico design of a TLR4-mediating multiepitope chimeric vaccine against amyotrophic lateral sclerosis via advanced immunoinformatics. J Leukoc Biol. 2022 Nov;112(5):1191–207.
68. Kak G, Raza M, Tiwari BK. Interferon-gamma (IFN-γ): Exploring its implications in infectious diseases. Biomol Concepts. 2018 May;9(1):64–79.
69. Muñoz-Fernández MA, Fernández MA, Fresno M. Activation of human macrophages for the killing of intracellular Trypanosoma cruzi by TNF-alpha and IFN-gamma through a nitric oxide-dependent mechanism. Immunol Lett. 1992 Jun;33(1):35–40.
70. Ruegemer JJ, Ho SN, Augustine JA, Schlager JW, Bell MP, McKean DJ, et al. Regulatory effects of transforming growth factor-beta on IL-2- and IL-4-dependent T cell-cycle progression. J Immunol. 1990 Mar;144(5):1767–76.
71. Gigoux M, Lovato A, Leconte J, Leung J, Sonenberg N, Suh WK. Inducible costimulator facilitates T-dependent B cell activation by augmenting IL-4 translation. Mol Immunol. 2014 May;59(1):46–54.
72. Barancheshmeh M, Najafzadehvarzi H, Shokrzadeh N, Aram C. Comparative Analysis of Fennel Essential Oil and Manganese in PCOS Rat Model via modulating miR-145 Expression and Structure-Based Virtual

Screening of IGF2R Protein to Address Insulin Resistance and Obesity. Obes Med. 2024;100574.
73. Ullah A, Ahmad S, Ismail S, Afsheen Z, Khurram M, ul Qamar M, et al. Towards A Novel Multi-Epitopes Chimeric Vaccine for Simulating Strong Immune Responses and Protection against Morganella morganii. Int J Environ Res Public Health. 2021;18(20).
74. Khan S, Irfan M, Hameed AR, Ullah A, Abideen SA, Ahmad S, et al. Vaccinomics to design a multi-epitope-based vaccine against monkeypox virus using surface-associated proteins. J Biomol Struct Dyn. 2022 Dec;1–10.
75. Aram C, Alijanizadeh P, Saleki K, Karami L. Development of an ancestral DC and TLR4-inducing multi-epitope peptide vaccine against the spike protein of SARS-CoV and SARS-CoV-2 using the advanced immunoinformatics approaches. Biochem Biophys Rep. 2024;39:101745.
76. Van Der Spoel D, Lindahl E, Hess B, Groenhof G, Mark AE, Berendsen HJC. GROMACS: fast, flexible, and free. J Comput Chem. 2005 Dec;26(16):1701–18.
77. López-Blanco JR, Aliaga JI, Quintana-Ortí ES, Chacón P. iMODS: internal coordinates normal mode analysis server. Nucleic Acids Res. 2014 Jul;42(Web Server issue):W271-6.
78. Seyfi S, Azadmehr A, Ezoji K, Nabipour M, Babazadeh A, Saleki K, et al. Mortality in ICU COVID-19 Patients Is Associated with Neutrophil-to-Lymphocyte Ratio (NLR): Utility of NLR as a Promising Immunohematological Marker. Interdiscip Perspect Infect Dis. 2023;2023(1):9048749.
79. Saleki K, Payandeh P, Shakeri M, Pourahmad R, Banazadeh M, Alijanizadeh P, et al. Utilizing immunoinformatics to target brain tumors; an aid to current neurosurgical practice. Interventional Pain Medicine and Neuromodulation. 2022;2(1).
80. Firuzpour F, Saleki K, Aram C, Rezaei N. Nanocarriers in glioblastoma treatment: a neuroimmunological perspective. Rev Neurosci. 2024;(0).
81. Saleki K, Shirzad M, Banazadeh M, Mohamadi MH, Alijanizadeh P, Javanmehr N, et al. Lupus and the nervous system: a neuroimmunoloigcal update on pathogenesis and management of systemic lupus erythematosus with focus on neuropsychiatric SLE. In: Systemic Lupus Erythematosus-Pathogenesis and Management. IntechOpen; 2022.
82. Aram C, Alijanizadeh P, Saleki K, Karami L. Development of an ancestral DC and TLR4-inducing multi-epitope peptide vaccine against the spike protein of SARS-CoV and SARS-CoV-2 using the advanced immunoinformatics approaches. Biochem Biophys Rep. 2024;39:101745.
83. Saleki K, Banazadeh M, Saghazadeh A, Rezaei N. Aging, testosterone, and neuroplasticity: friend or foe? Rev Neurosci. 2023;34(3):247–73.
84. Saleki K, Mohamadi MH, Alijanizadeh P, Rezaei N. Neurological adverse effects of chimeric antigen receptor T-cell therapy. Expert Rev Clin Immunol. 2023;19(11):1361–83.
85. Abdi SAH, Ali A, Sayed SF, Abutahir, Ali A, Alam P. Multi-Epitope-Based Vaccine Candidate for Monkeypox: An In Silico Approach. Vaccines (Basel). 2022 Sep;10(9).
86. Saleki K, Payandeh P, Shakeri M, Pourahmad R, Banazadeh M, Alijanizadeh P, et al. Utilizing Immunoinformatics to Target Brain Tumors; An Aid to Current Neurosurgical Practice. Interventional Pain Medicine and Neuromodulation. 2022;2(1).
87. Tomar N, De RK. Immunoinformatics: a brief review. Methods Mol Biol. 2014;1184:23–55.
88. Guo N, Niu Z, Yan Z, Liu W, Shi L, Li C, et al. Immunoinformatics Design and In Vivo Immunogenicity Evaluation of a Conserved CTL Multi-Epitope Vaccine Targeting HPV16 E5, E6, and E7 Proteins. Vaccines (Basel). 2024 Apr;12(4).
89. Saleki K, Alijanizade P, Moradi S, Rahmani A, Banazadeh M, Mohamadi MH, et al. Engineering a novel immunogenic chimera protein utilizing bacterial infections associated with atherosclerosis to induce a deviation in adaptive immune responses via Immunoinformatics approaches. Infection, Genetics and Evolution. 2022;102:105290.
90. Saleki K, Shirzad M, Javanian M, Mohammadkhani S, Alijani MH, Miri N, et al. Serum soluble Fas ligand is a severity and mortality prognostic marker for COVID-19 patients. Front Immunol. 2022;13:947401.
91. Rahmani A, Baee M, Saleki K, Moradi S, Nouri HR. Applying high throughput and comprehensive immunoinformatics approaches to design a trivalent subunit vaccine for induction of immune response against emerging human coronaviruses SARS-CoV, MERS-CoV and SARS-CoV-2. J Biomol Struct Dyn. 2022;40(13):6097–113.
92. Aram C, Alijanizadeh P, Saleki K, Karami L. Development of an ancestral DC and TLR4-inducing multi-epitope peptide vaccine against the spike protein of SARS-CoV and SARS-CoV-2 using the advanced immunoinformatics approaches. Biochem Biophys Rep. 2024;39:101745.
93. Saleki K, Aram C, Alijanizadeh P, Khanmirzaei MH, Vaziri Z, Ramzankhah M, et al. Matrix metalloproteinase/Fas ligand (MMP/FasL) interaction dynamics in COVID-19: An in silico study and neuroimmune perspective. Heliyon. 2024;10(10).
94. Latifi R, Azadmehr A, Mosalla S, Saleki K, Hajiaghaee R. Scolicidal effects of the Nicotiana tabacum L. extract at various concentrations and exposure times. J Med Plants. 2022;21(82):111–8.
95. Rong H guo, Zhang X wen, Han M, Sun X, Wu X dan, Lai X zhen, et al. Evidence synthesis of Chinese medicine for monkeypox: Suggestions from other contagious pox-like viral diseases. Front Pharmacol. 2023;14:1121580.
96. Vaziri Z, Saleki K, Aram C, Alijanizadeh P, Pourahmad R, Azadmehr A, et al. Empagliflozin treatment of cardiotoxicity: A comprehensive review of clinical, immunobiological, neuroimmune, and therapeutic implications. Biomedicine & Pharmacotherapy. 2023;168:115686.